UPPSALA
UNIVERSITET

Digital Comprehensive Summaries of Uppsala Dissertations from the Faculty of Science and Technology 212

Applications of Gamma Ray Spectroscopy of Spent Nuclear Fuel for Safeguards and Encapsulation

CHRISTOFER WILLMAN

ACTA
UNIVERSITATIS
UPSALIENSIS
UPPSALA
2006

ISSN 1651-6214
ISBN 91-554-6637-0
urn:nbn:se:uu:diva-7116

Dissertation presented at Uppsala University to be publicly examined in Polhemsalen, Ångströmlaboratoriet, Uppsala, Friday, September 29, 2006 at 09:00 for the degree of Doctor of Philosophy. The examination will be conducted in English.

Abstract
Willman, C. 2006. Applications of Gamma Ray Spectroscopy of Spent Nuclear Fuel for Safeguards and Encapsulation. Acta Universitatis Upsaliensis. *Digital Comprehensive Summaries of Uppsala Dissertations from the Faculty of Science and Technology* 212. 81 pp. Uppsala. ISBN 91-554-6637-0.

Nuclear energy is currently one of the world's main sources of electricity. Closely connected to the use of nuclear energy are important issues such as the nonproliferation of fissile material that may potentially used in nuclear weapons (safeguards), and the management of the highly radioactive nuclear waste. This thesis addresses both these issues by contributing to the development of new experimental methods for ensuring safe and secure handling of the waste, with focus on methods to be used prior to encapsulation and final storage.

The methods rely on high resolution gamma ray spectroscopy (HRGS), involving the measurement and analysis of emitted gamma radiation from the fission products ^{137}Cs, ^{134}Cs and ^{154}Eu. This technique is nondestructive, making it relatively nonintrusive with respect to the normal operation of the nuclear facilities.

For the safeguards issue, it is important to experimentally verify the presence and identity of nuclear fuel assemblies and also that the fuel has experienced normal, civilian reactor operation. It has been shown in this thesis that the HRGS method may be used for verifying operator declared fuel parameters such as burnup, cooling time and irradiation history. In the experimental part of the work, the burnup and the cooling time has been determined with an accuracy of 1.6% and 1.5%, respectively (1 σ).

A technique has also been demonstrated, utilizing the ratio ^{134}Cs/^{154}Eu, with which it is possible to determine whether a fuel assembly is of MOX or LEU type. This is of interest for safeguards as well as for the safe operation of a final storage facility.

As an improvement to the HRGS technique, measuring a part of the fuel assembly length in order to reduce measurement time has been suggested and investigated. A theoretical case for partial defect verification has also been studied as an extension of the HRGS technique.

Finally, HRGS has been used for determining the decay heat in spent nuclear fuel assemblies, which is of importance for the safe operation of a final storage facility. This application is based on the radiation from ^{137}Cs, and the accuracy demonstrated was within 3% (1 σ).

Keywords: gamma radiation, spectroscopy, spent nuclear fuel, safeguards, HRGS, MOX

Christofer Willman, Department of Nuclear and Particle Physics, Box 535, Uppsala University, SE-75121 Uppsala, Sweden

ISSN 1651-6214
ISBN 91-554-6637-0
urn:nbn:se:uu:diva-7116 (http://urn.kb.se/resolve?urn=urn:nbn:se:uu:diva-7116)

To my family

List of papers

This thesis is based on the following papers, which are referred to in the text by their Roman numerals.

I C. Willman, A. Håkansson, O. Osifo, A. Bäcklin and S. Jacobsson Svärd (2006) Nondestructive assay of spent nuclear fuel with gamma-ray spectroscopy.
Annals of Nuclear Energy, 33(5):427-438

II C. Willman, A. Håkansson, O. Osifo, A. Bäcklin and S. Jacobsson Svärd (2006) A nondestructive method for discriminating MOX fuel from LEU fuel for safeguards purposes.
Annals of Nuclear Energy, 33(9):766-773

III C. Willman, A. Håkansson, S. Jacobsson Svärd, O. Osifo and A. Bäcklin (2006) Improved gamma ray spectroscopy of spent PWR nuclear fuel.
To be submitted to Annals of Nuclear Energy

IV O. Osifo, C. Willman, A. Håkansson, S. Jacobsson Svärd, A. Bäcklin and T. Lundqvist (2006) Verification and determination of the decay heat in spent PWR fuel by means of gamma scanning.
To be submitted to Nuclear Science and Engineering

Author's comments regarding the papers

Papers I, II and III were analysed from experimental data obtained by the author and written by the author. Paper IV was mainly written by O. Osifo but the author was involved in the data collection, as well as in the analysis and proof reading. Paper I and Paper II were refereed by the reviewers of the Elsevier Journal Annals of Nuclear Energy.

The papers are ordered chronologically according to their respective publication date, where applicable.

Complementary paper not included in the thesis

In addition to the presented papers, the author has contributed and/or written the following papers.

I C. Willman, O. Osifo, A. Håkansson and S. Jacobsson Svärd (2005) A Semi-Empirical Technique for Verification of Spent Nuclear Fuel Assemblies.
27^{th} Annual Symposium on Safeguards and Nuclear Materials Management (ESARDA) London, UK, May 10-12

II S. Jacobsson Svärd, A. Håkansson, A. Bäcklin, P. Jansson, O. Osifo and C. Willman (2006) Tomography for partial defect verification – experiences from measurements using different devices.
ESARDA Bulletin No. 33, February 2006, pp. 15-25. ISSN: 0392-3029

III S. Jacobsson Svärd, A. Håkansson, A. Bäcklin, O. Osifo, C. Willman and P. Jansson (2005) Nondestructive Experimental Determination of the Pin-Power Distribution in Nuclear Fuel Assemblies.
Nuclear Technology vol. 146, no. 1, April 2004, pp. 58-64. ISSN: 0029-5450

IV S. Jacobsson Svärd, A. Håkansson, A. Bäcklin, O. Osifo, C. Willman and P. Jansson (2003) Non-destructive experimental determination of the pin-power distribution in nuclear fuel.
3^{rd} Meeting on Advances in Nuclear Fuel Management (ANFM III) Hilton Head Island, SC, USA, October 5-8

Author's comments regarding the complimentary papers

Paper I was prepared and written by the author, for the remaining Papers II, III and IV, the author contributed to the experimental work and proof reading of the papers.

Contents

Abbreviations

b	Barn. A unit for cross section of nuclear reactions, 1 b=10^{-28} m^2. Can be interpreted in terms of probability.
BU	Burnup. The total amount of energy produced in a nuclear fuel, often expressed in GWd/tU.
BWR	Boiling water reactor.
CLAB	Centralt mellanlager för använt kärnbränsle. The Swedish interim storage for spent nuclear fuel.
CT	Cooling time. The time passed since the fuel assembly was taken out of the reactor core.
GWd/tU	Gigawatt days of thermal energy produced per tonne uranium initially present in the fuel. A unit of burnup.
HRGS	High resolution gamma ray spectroscopy.
IAEA	The International atomic energy agency.
IEA	The International energy agency.
keV	Kilo electron volt. The unit used to quantify photon energy.
LWR	Light water reactor.
MOX	Mixed oxide fuel. A reprocessed fuel that contains a mixture of uranium and plutonium oxide.
PWR	Pressurized water reactor.
SKB	Svensk kärnbränslehantering. The Swedish nuclear fuel and waste management company. Responsible for the final deposition of spent nuclear fuel in Sweden.
SKI	The Swedish nuclear power inspectorate.
UN	United nations.

1. Introduction

This thesis consists of a comprehensive summary based on four scientific papers all focusing on nondestructive high resolution gamma ray spectroscopy measurements. The methods described have been developed for Swedish operating conditions using existing equipment although they can be applied generally.

1.1 Short account on the history of nuclear energy

In 1942, Enrico Fermi first managed to control a sustained nuclear fission process in a small graphite moderated reactor which ran for about four and a half minute, producing one half watt of power. For the first time, it was shown that a rector could be started and stopped at will.

This construction with a moderator and fuel organized in a lattice prompted new reactor designs that eventually led to constructions capable of producing significant amounts of plutonium for the "Manhattan" project and three years later two nuclear bombs were dropped over Japan, marking the end of the second world war.

The following years saw intensive efforts to prevent proliferation of nuclear technology. This "policy of denial" was mainly controlled by embargo measures. However, both the Soviet Union and the United Kingdom were considered nuclear states a few years after the USA since these states then had both nuclear power and nuclear explosives.

The policy of denial was considered inefficient since it was realized that any state with a reasonable level of industrial base would be able to acquire nuclear explosives. The introduction of new nuclear states on the scene could furthermore alter the "balance of terror" in a nonpredictable way. This all led to the abandoning of the policy of denial in favour of the opposite policy of cooperation.

In December 1953, president Eisenhower of USA presented the "Atoms for peace" programme to the United Nations. The policy of denial was now changed to a liberal exportation of nuclear technology. However, the receiving states of this nuclear technology were all obliged to the restriction of not using the nuclear technology for military purposes. As a consequence of this, the International Atomic Energy Agency (IAEA) was formed in 1957, within the United Nations family, to verify that these commitments of the receiving countries all were held.

Two main objectives for the IAEA were formulated.

- Worldwide promotion of civil nuclear technology.
- Safeguarding the promoted nuclear technology to ensure the nonproliferation of nuclear weapons.

The IAEA came to hold a unique position and through bilateral agreements, the IAEA could demand insight to a State's nuclear material, technology and future ambitions regarding nuclear technology actions. The agreements also specify that the IAEA has access to a State's nuclear facilities where inspections may be performed in the areas normally classified as national security.

The ratification of the treaties is on a basis of free-willingness and the States issues general invitations to IAEA to perform inspections. The IAEA cannot force a State to accept inspections, nor can the IAEA issue sanctions on its own. However, a State that refuses to submit to inspections may be subject for sanctions issued by the UN.

1.2 Nuclear safeguards

Safeguards performed by the IAEA was at first focused on suppliers of technology and knowledge. It was however concluded that this approach was not sufficient and more elaborate safeguards activities were necessary to keep up with the general development of society and technology. The revised safeguards thus included all activities related to any form of nuclear technology.

The famous "Treaty on the Non-Proliferation of Nuclear weapons" (NPT) was issued in June 1968 and came into force in March 1970. This treaty regulated that the undersigned States commit themselves not to divert nuclear material from peaceful uses to nuclear explosives. The treaty has become one of the most important and powerful tools in the realm of nuclear arms control.

The two cornerstones of the IAEA's activities are the IAEA information circular INFCIRC and the NPT. The INFCIRC describes the definitions, goals, means and other relevant information to ensure that safeguards is performed coherently wherever it is done.

As of March 2002, 187 States have ratified the NPT, including the five classical nuclear weapon States, USA, Russian Federation, UK, France and China. An indication of the significance of the NPT is that more countries have ratified the treaty than any other arms limitation and disarmament agreement. The two goals of the NPT are that it should prevent the diversion of fissile material for weapons use through safeguards and that it should promote cooperation regarding peaceful nuclear technology and equal access to this technology for all States included in the NPT. It can be noted that the NPT declares that it should not affect the development of nuclear

technologies for peaceful use. Furthermore, the NPT declares that it is not allowed for any State to provide material or technology to a non nuclear State, even for peaceful use, unless it is subject to safeguards.

To strengthen the safeguards system, the need for creating additional sources of information has been identified. Therefore, the Additional Protocol [1] has been issued. The Additional Protocol is a legal document granting the IAEA complementary inspection authority to that provided in underlying safeguards agreements. A principal aim is to enable the IAEA inspectorate to provide assurance about both declared and possible undeclared activities. The Additional Protocol grants IAEA expanded rights of access to information and sites, as well as additional authority to use the most advanced technologies during the verification process. As a few examples, the Additional Protocol gives the IAEA access to any location where nuclear material is or may be present and collection of environmental samples at locations beyond declared locations.

To verify that all protocols and agreements are held, it is obvious that the IAEA needs to perform inspections and measurements. Facilities of interest in this context are e.g. mines, fuel factories, reprocessing plants, spent fuel storages and nuclear power plants, but also facilities handling and manufacturing special alloys, electronics or other products that may have a relevance for safeguards.

Inspections are carried out at a defined schedule but also at short notice. The IAEA inspectors perform various activities during and in connection with on site inspections or visits at the facilities. The inspections may include auditing the facility's accounting and operating records and comparing these records with the State's accounting reports to the IAEA. Basically, the inspections comprise two main areas [2].

Accountancy States are obliged to report the possession of its nuclear material. All processing and import and export of nuclear material and materials specially designed for nuclear technology use are subject to reporting. The objective for inspections is to quantitatively determine the amount of material actually present and compare with the State's declared amount, i.e. verifying the operator declared data. The ultimate goal is thus to ensure that no fissile material or other relevant items are missing.

Containment and surveillance (C/S) To verify the integrity of e.g. canisters or buildings, various types of seals are used. Photographic films and TV-cameras are, for instance, used for surveying specific areas of nuclear facilities. During inspections seals are checked and films and videotapes are examined.

The technical means of performing the inspections can be carried out with destructive assay (DA) or non destructive assay (NDA). Destructive assay is a somewhat complicated procedure since the measured object is, as

the name suggests, destroyed and special laboratories are needed. On the other hand, the information gained using DA is in general of a very high quality. One obvious reason why NDA may be preferred for in field inspections is that it offers the possibility to extract information without destroying the object of interest and also that it gives minimal interference with regular activities at the facility. The latter is an important aspect since the acceptance to new safeguards measures among operators in many cases depends on that smooth, efficient and cost effective inspections can take place.

Apart from IAEA inspections, there are also additional authorities for each country. Being a member of the European union, Sweden has given the EU the right to perform inspections via Euratom, inspection body in the European region. Sweden has an inspecting organization on its own, the Nuclear Power Inspectorate (Statens kärnkraftsinspektion, SKI). SKI is responsible for national safeguards inspections and also checks that the Swedish nuclear power plants are operated as stated. Moreover, SKI is a driving force for nuclear security development.

2. Nuclear energy and the nuclear fuel cycle

2.1 Nuclear energy

Nuclear energy is supplying the world with around 20% of the electric energy from about 440 reactors. In Sweden, ten reactors are in operation, providing about half of the electric energy used in a year.

The International Energy Agency, IEA, predicts that the energy demand will grow with about 2/3 in the coming 20-30 years [3]. Many countries, mainly in Asia, are planning or considering nuclear energy as their source of electric energy for the nearest future. In Europe, Finland is currently constructing a new power plant, which is expected to be in operation around 2010.

A nuclear power plant is built to utilize the released energy in the *fission* process, see section 3.4.1. When fission occurs, the released energy is transformed mainly into heat. This heat is used to boil water, so a nuclear power plant can be seen as a big construction for boiling water. The boiling water produces steam, which is fed into a turbine system, which in turn is connected to a generator that produces electric power. The water used is usually ordinary water but there are few reactor designs using heavy water[1]. In this respect, ordinary water is light and the reactor type using ordinary water are called light water reactors (LWR).

Fission of uranium is a very energy rich process, for comparison, 1 kg uranium contains the energy equivalent of 90 tonne of coal.

LWR nuclear reactors are of mainly two different types, Boiling Water Reactors (BWR) and Pressurized Water Reactors (PWR), where the vast majority of the world's reactors are PWRs. In a PWR reactor the heated water is pressurized and is thus prevented from boiling. The steam is instead created in an isolated adjacent system, where the heated water is allowed to interact through heat exchangers producing steam.

In a BWR reactor, the heated water is allowed to boil in the reactor core and then fed to the turbines for electric power generation. After the steam has passed the turbines, it is condensed and fed back as water again into the core and the boiling process is repeated.

[1] Heavy water, D_2O, water that contains heavy hydrogen, deuterium, instead of ordinary hydrogen.

Apart from these two reactor types it is also worth mentioning the graphite moderated RBMK reactors, more known as the Chernobyl reactor type, where the graphite serves as the moderator. Canada uses the CANDU reactor for energy production which is a reactor using heavy water as moderator. Both these types of reactors can be operated using natural uranium and/or uranium with a low enrichment of ^{235}U. Other more exotic reactor designs have also been used but to a smaller extent.

Research is still being performed and South Africa has designed a new reactor called the pebble-bed reactor [4]. The next step in reactor development has now been taken by ten countries with the Generation IV initiative [5]. For the work of Generation IV, six new reactor types are presented. These reactors are designed to use natural resources optimally and to address safety issues, waste and proliferation resistance.

2.2 The Swedish nuclear fuel cycle

In Sweden, the use of nuclear fuel is based on the once through principle, meaning that uranium is mined, converted into fuel assemblies, used for power production and eventually stored in a final repository. The name once through refers to that no reprocessing of the spent fuel assemblies is done. A brief description of the different parts of the once through process follows.

Mining, conversion and fuel fabrication Uranium is mined in some 20 countries, primarily in Canada and Australia. About half the annual demand comes from mines but considerable quantities also comes from Russian weapons stockpiles - recycled warheads [6]. When the uranium has been mined it is converted into gaseous uranium hexafluoride, UF_6, at a conversion plant. Natural uranium consists of 0.72% ^{235}U and 99.27% ^{238}U and the UF_6 must be enriched to a few percent in ^{235}U before it can be used for power production in LWRs. Enrichment is often done by gaseous diffusion where the UF_6 passes through a long series of filters that allows the lighter ^{235}U to pass through faster than the ^{238}U. After enrichment about 15% of the original quantity of the UF_6 is available as enriched uranium. The remains are rejected as tails and stockpiled. Enrichment is for instance done at the Tricastin enrichment plant in France.

The enriched uranium is converted to uranium dioxide, UO_2, and sintered to fuel pellets. The pellets are stacked in tubes and mounted to fuel assemblies. This type of fuel fabrication is for instance done in Västerås in Sweden. The steps above are known as the front end of the fuel cycle.

Power production Sweden has ten reactors currently in operation, seven BWRs and three PWRs. Each reactor uses between 160 - 650 fuel assemblies depending on reactor type. In Sweden, a fuel assembly undergoes irradiation for approximately 11 months before the reactor is shut down for maintenance and refuelling. Each fuel assembly is used for power production for 4 - 5 years before it is considered fully used. Consequently, about 20% of the assemblies are removed from the core each year.

Interim storage and final storage When the fuel assemblies have been removed from the core they are usually stored on-site for one year before they are moved to the central interim storage, CLAB, in Oskarshamn. The spent fuel assemblies are stored in water which provides both cooling and radiation shielding. Here, the assemblies will cool for another 30 - 40 years. Finally, the fuel assemblies will be deposited in the bedrock, as described in section 2.4.

2.3 Reprocessing and utilization of MOX fuel

MOX fuel is a type of nuclear fuel that is made from recycling spent uranium fuel. In ordinary fuel, a number of plutonium isotopes are formed due to neutron capture in ^{238}U after which ^{239}Pu is formed via two beta decay steps. If ^{239}Pu absorbs one or more neutrons ^{240}Pu, ^{241}Pu and ^{242}Pu are formed. After a nuclear fuel assembly has been discharged about half of the ^{239}Pu produced during irradiation has been "burned". This contributes with approximately one third of the total energy. Spent nuclear fuel consists of one percent plutonium, two thirds of this being the fissile isotopes ^{239}Pu and ^{241}Pu.

At a reprocessing plant, the plutonium is separated from the remaining uranium and is later mixed as an oxide with depleted uranium to form the new MOX fuel in the form UO_2+PuO_2. MOX is hence short for Mixed Oxide fuel. Typical MOX fuel contains plutonium to about 5 - 9 % which corresponds to a uranium enrichment of 3 - 5 %. This difference is because not all of the plutonium isotopes are fissile. A reactor can be loaded with up to 50% MOX fuel but most reactors using MOX fuel are loaded to one third with MOX fuel in the core.

MOX fuel can also be made from the plutonium contained in nuclear weapons. The objective with this is to convert the weapons grade plutonium into reactor grade plutonium and thereby reducing the amount of fissile material suitable for weapons use[2].

[2]Reactor grade plutonium has a higher content of ^{240}Pu which is an undesired isotope for use in nuclear weapons due to spontaneous fission. The spontaneous fission also causes a heat removal problem.

The use of MOX fuel is expected to significantly reduce plutonium inventories. As an example, the Euratom Supply Agency estimates that the use of a single MOX fuel element consumes 9 kg of plutonium, and avoids the production of a further 5 kg (compared with the use of low enriched uranium fuel). Thus, in this example, each MOX fuel element used results in a net reduction of 14 kg of plutonium.

2.4 Encapsulation and final storage

In Sweden, the producers of nuclear energy are all obliged to produce a waste disposal plan for the spent nuclear fuel. In the seventies, the owners of the nuclear power plants formed Svensk kärnbränslehantering AB, SKB, as their means to fulfil the waste disposal issue. The current plan is that the nuclear waste shall be taken care of according to the KBS-3 method [7].

The KBS-3 method for final storage of spent fuel is based on a geological repository located at a depth of about 500 m into the bedrock. The assemblies will be encapsulated in canisters made of copper equipped with a steel insert. Copper is chosen due to the good corrosion properties and the steel insert for mechanical stability [8].

The canisters will be embedded in bentonite clay, which expands greatly when it absorbs water. The bentonite prevents direct water flow onto the canister, and protects it from minor bedrock movements through its deformation. The bentonite clay will loose its properties if it is heated above 100° C, and the surface temperature of the canisters must therefore be limited to this temperature. Accordingly, there is an upper limit of the total decay heat of the fuel assemblies placed in the canister, which is about 1700 W [9]. To minimize the number of canisters used, it is of importance to fill the canisters with as many assemblies as possible, within the design limit. The spent fuel assemblies therefore need to be controlled with regard to the decay heat so this requirement is met. A spent BWR assembly will have a decay heat in the order of about 100 W and a PWR assembly about 500 W, both after a cooling time of approximately 40 years.

When the last canister is in place, the repository will be sealed. The KBS-3 system is designed to safely keep the radioactive material from the biosphere until the radiation level has reached that of natural uranium ore, which requires a storage time of the order of 100 000 years.

3. Properties of spent nuclear fuel

For the Swedish types of reactors two different fuel types exist, one for BWR reactors and one for PWR reactors and there are a number of different physical properties of these two fuel types which will be described below. For the fission process to be self sustained, the fuel is designed to obtain a suitable fuel-to-water ratio. This is done by stacking pellets of fuel into tubes. These fuel rods have a diameter of about one centimeter and are mounted in a quadratical pattern to form a fuel assembly. By using appropriate spacings between the fuel rods, the neutrons will be moderated by the water, i.e. slowed down, before they enter an adjacent fuel rod and induce further fissions.

3.1 Physical properties of nuclear fuel assemblies

For BWR fuel elements, about 100 fuel rods are used and for a PWR fuel approximately 300 fuel rods make up the assembly, depending on the fuel design. The BWR fuel rods are surrounded by a channel with the purpose of directing water through the assembly, see figure 3.1.

For a PWR assembly this channel is not needed because no boiling occurs. The weight of a BWR assembly is approximately 200 kg and for a PWR assembly it is about 300 kg. The physical dimensions for a BWR and a PWR is $140 \times 140\,\mathrm{mm}^2$ and $210 \times 210\,\mathrm{mm}^2$, respectively. The two fuel types both have a length of about 4 m. In figure 3.2 an illustration of a PWR fuel assembly is shown.

Since the reactor is designed to produce heat, the fuel must have a high melting point and high thermal conductivity. It should also be insensitive to radiation damage and be chemically inert. The fuel pellets are therefore made of ceramic UO_2 which fulfills these requirements, although the thermal conductivity is quite low. This fuel type is often referred to as Low Enriched Uranium fuel or LEU fuel. The tubes containing the pellets are made of a Zirconium alloy, which offers good mechanical stability and at the same time low neutron absorption. The cross sections showing the fuel rod configuration of the two fuel types can be seen in figure 3.3 and 3.4.

Figure 3.1: Illustration of a BWR fuel assembly with the fuel channel visible on the left side. Reproduced with courtesy of Westinghouse Electric Sweden AB.

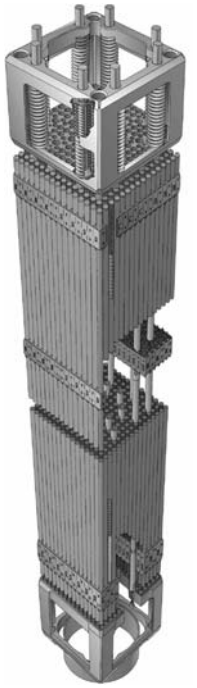

Figure 3.2: Illustration of a PWR fuel assembly. Here, no fuel channel is needed. Reproduced with courtesy of Westinghouse Electric Sweden AB.

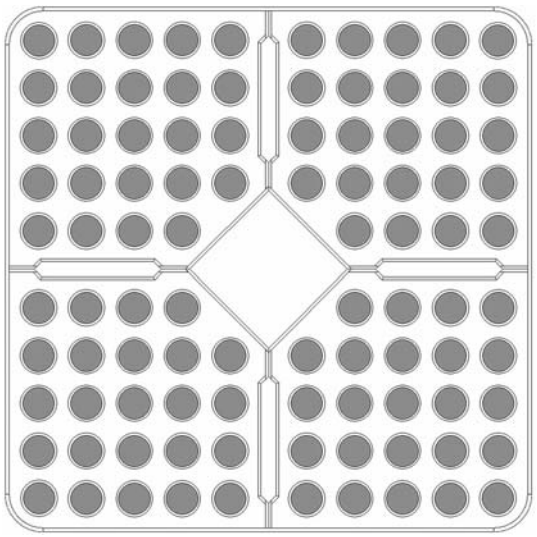

Figure 3.3: The cross section of a BWR SVEA-96S type, with 96 fuel rods (grey). A water channel can be seen in the center of the fuel assembly.

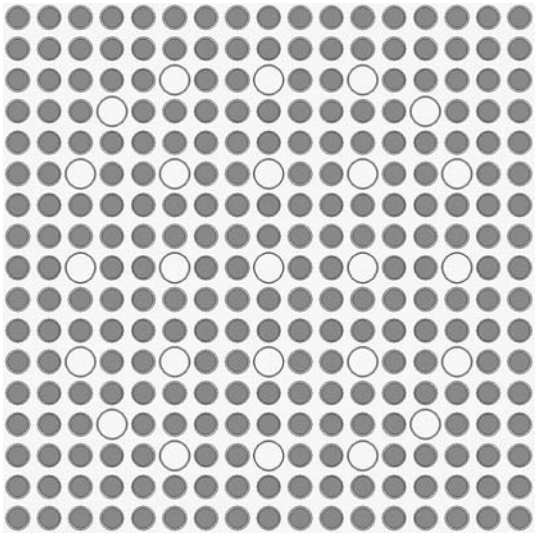

Figure 3.4: The cross section of a PWR 17 × 17 type with 264 fuel rods (grey) and 25 guide tubes (white).

3.2 Control blades and rods

Intimately associated with nuclear fuel are the control blades or control rods for a BWR reactor and a PWR reactor, respectively. The control blades and control rods have the same function but are designed differently depending on reactor type. Their purpose is to absorb neutrons efficiently and they are used for controlling the reactor power level. They are also used for safety reasons, such as if a quick shutdown of the reactor is necessary. The materials used in the control blades/rods contain strongly neutron absorbing elements, most often boron carbide and hafnium. See figure 3.5 for two types of control blades for BWR reactors.

When a core is loaded with MOX fuel, more control blades need to be added. This is mainly due to the fact that plutonium has fewer delayed neutrons as compared to uranium, see section 3.4.1. Moreover, ^{239}Pu has a higher absorption cross section for thermal neutrons compared to ^{235}U, and the average energy of the neutron spectrum in reactors using plutonium fuels is higher. This causes the capture of neutrons by control rods to be reduced if plutonium fuel is used, thus further reducing the effectiveness of the control blades.

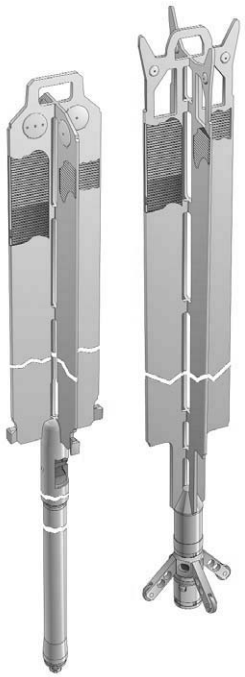

Figure 3.5: Illustration of two types of control blades for a BWR reactor. Reproduced with courtesy of Westinghouse Electric Sweden AB.

3.3 Parameters of spent nuclear fuel

A spent nuclear fuel assembly is characterized by a number of parameters and a few of safeguards relevance are described below.

Burnup (BU) This quantity describes the total energy produced in the fuel. It is often expressed in giga watt days per tonne uranium [GWd/tU] which expresses the integrated energy over time.

Cooling time (CT) The time passed since the assembly was taken out of the core. Typical cooling times in this thesis range from 10 - 20 years.

Initial enrichment The amount of ^{235}U present in the fuel before irradiation, usually between 1.5% - 4% by weight but the increasing energy demand has driven the world average enrichment from 3.35% in 1990 to an expected 3.85% in 2010. Much care is taken when designing nuclear fuel, with many rods having different enrichments. This is done to get a homogenously distributed power throughout the reactor core. BWR fuel assemblies may for instance have a lower enrichment in the fuel periphery to achieve a good neutron economy.

Irradiation history A detailed description on how the burnup is distributed in time. For safeguards reasons it may be of importance to verify that an irradiation history is compatible with the expected civilian use of the reactor. Unusually short fuel cycles at low neutron fluxes produces more plutonium with a quality better suited for weapons production than a normal fuel cycle which is used in reactors for power production.

Decay heat The heat of a spent nuclear fuel assembly. The decay heat is produced, as the name suggests, from mainly decaying fission fragments. The decay heat has implications on how to design and to dimension possible final repositories.

In this context, *void* should also be mentioned. Void is defined as the volume fraction of steam in a steam-water mixture. The void must be taken into account for BWR reactors where the boiling water creates the void. Void is a poor moderator and the reactor power is thus dependent on the void. Also, the isotopic composition of the fuel is affected by the void. For a BWR reactor, the average void is somewhere around 40 - 50%.

3.4 Isotopic content of spent fuel

3.4.1 The fission process

Nuclear energy is based on a neutron splitting a heavy nucleus into smaller parts, fission, which generates large amounts of energy. In a nuclear reactor,

uranium (U), and especially ^{235}U, is the primary source of energy. The fission process is a self sustaining process meaning that for every fission, 2 - 3 new neutrons are released which in turn can create fissions in surrounding uranium atoms. A newly released neutron needs to be slowed down (moderated) in order to have the highest probability to create an additional fission. Water is used for this task (moderation), neutrons travelling through water will eventually be slowed down. At the same time water is used to transport the heat out from the reactor and thus the water serves two purposes.

As mentioned previously, an average fuel assembly consists of ^{238}U to about 96% and ^{235}U to 4% when the fuel is inserted into the reactor core. In a BWR reactor the fuel assembly is exposed to a thermal neutron flux density of $\sim 10^{14}$ n/s/cm^2. Fissions will be induced by the neutrons, and as a result, creating fission products. These fission products have a mass distribution according to figure 3.6. It can be seen that there is a high probability for creating fission products with masses around 95 and 140. It can also be

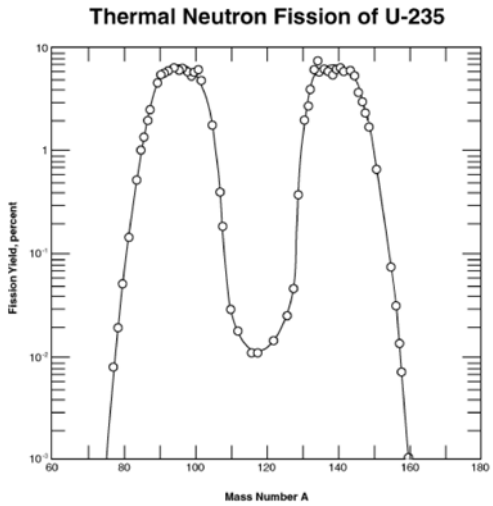

Figure 3.6: Mass distribution of fission fragments from thermal-neutron induced fission of ^{235}U.

noticed that it is not very likely that two fission fragments with equal masses are formed. However, it has been seen that for high energy fission, i.e. fast neutrons, fission fragments of equal mass are more probable [10].

The fission fragments exhibit a neutron excess making them unstable or *radioactive*. The nucleus of a fission fragment corrects this excess of energy by emitting neutrons and/or gamma rays.

Some fission fragments emit neutrons within 10^{-16} s. These neutrons are called prompt neutrons and for fission of ^{235}U, an average of 2.42 neutrons

are emitted for each fission. These neutrons can in turn create another fission in a surrounding ^{235}U nucleus and a chain reaction is maintained.

Some fission fragments also undergo β decay and this is sometimes followed by another neutron emission. These emitted neutrons are called delayed neutrons, where the term delayed relates to a period of time time, usually of the order of seconds.

The *half life* of a radioactive nucleus states the time for which it takes before half of the nuclei present from the beginning have decayed. Most fission products in a spent nuclear fuel decay within a few hours but some of the fission fragments have half lives that can be measured in days or years.

When the reactor is operating, the isotopic content of the fuel is, as described, gradually changing from only consisting of the two uranium isotopes to many other isotopes. At the end of the life of a fuel assembly, the fission rate percentage of ^{235}U has decreased from about 90% to 10%. ^{238}U contributes with around 10% throughout the fuel life by fast fission and the plutonium that has been built from capture reactions in ^{238}U contributes to the fission rate with about 80%.

3.4.2 Isotopes used in safeguards measurements

Since safeguards measurements should be done on fuel assemblies with short as well as long cooling times, the measurement methods should be based on isotopes with a long half life so a measurable signal can be acquired within a reasonably short time. The isotopes should also have an energy which is well separated from others so that spectrum evaluation can be made as accurately as possible and at the same time high enough to penetrate the fuel assembly. The isotopes studied in this thesis are shown in table 3.1.

Table 3.1: *The three isotopes studied in this work together with their gamma ray energies and half lives.*

Isotope	**Gamma-ray energy [keV]**	**Half life [years]**
^{134}Cs	796, 1365	2.1
^{137}Cs	662	30.1
^{154}Eu	1275	8.6

The energies listed are the ones most prominent in spent nuclear fuel. Beyond the listed energies it can be noted that both ^{134}Cs and ^{154}Eu radiate gamma quanta with additional energies but the intensities of these are relatively low. Other isotopes such as ^{140}Ba might be used but as the half life is only around 13 days it is, in practice, not measurable after only four months. This isotope is however used in tomographic measurements as it

is a good indicator for the thermal power distribution in fuel assemblies. A description of this can be found in [11].

To use the three isotopes presented in table 3.1 for safeguards applications it must be known how these are produced in the fuel during irradiation. This is accounted for in section 3.4.3 - 3.4.5.

3.4.3 The production of ^{137}Cs

As shown in figure 5.1, the largest peak in a typical measured spectrum is the one emanating from ^{137}Cs. The production path of ^{137}Cs is shown in figure 3.7, where the diagonal arrows represent β decay and the horizontal arrows represent neutron capture.

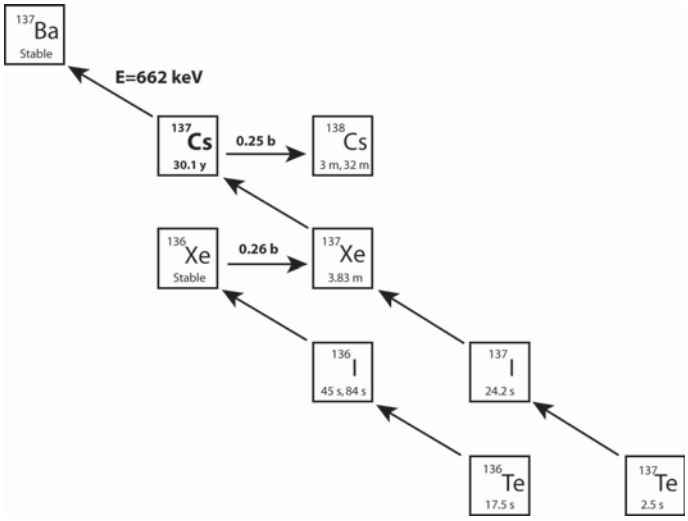

Figure 3.7: The production and decay of ^{137}Cs. The half lives and cross sections were taken from [12]. The gamma ray energy of ^{137}Cs is depicted in the figure.

It can be seen that mass chain 136 contributes to the production of ^{137}Cs with a neutron capture in ^{136}Xe. However, about the same amount that is produced this way is lost from neutron capture in ^{137}Cs, 0.26 b as compared to 0.25 b. From the production path it is anticipated that the ^{137}Cs should be produced linearly with the neutron flux and hence the burnup. Simulations with ORIGEN-ARP [13] have been made which show that this prediction is correct, the result can be seen in figure 3.8. The simulations were based on five cycles, each with an irradiation period of 335 days. Between each irradiation, a 30 day period shutdown was modelled when the fuel was not subject to any power production thus simulating the annual maintenance period.

The fission yields of ^{137}Cs are approximately the same for the fissile uranium and plutonium isotopes, see for instance [14]. The production is relative insensitive to irradiation history and initial enrichment, as a function

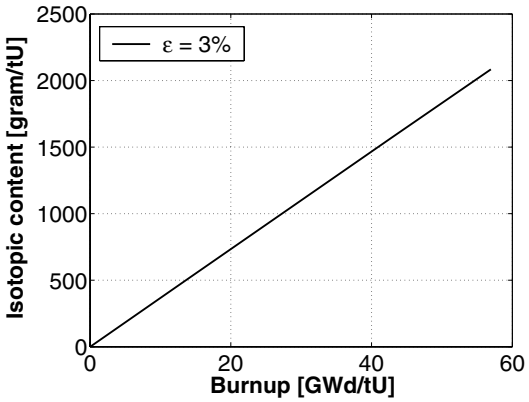

Figure 3.8: ^{137}Cs is produced linearly with burnup as this simulations shows. A 17×17 PWR fuel was used for the simulations with an initial enrichment of 3%. The deviation from linearity is 0.2%.

of burnup, and the long half life makes it suitable for use even after cooling times of several decades. Neither does the void have any significant effect on the production of ^{137}Cs.

It has been reported in [15] that ^{137}Cs migrates within the fuel pellets, both axially and radially but this effect was omitted in this work.

3.4.4 The production of ^{134}Cs

As figure 3.10 shows, the buildup of ^{134}Cs is more complicated than that of ^{137}Cs. It is primarily produced through resonance absorption of neutrons in the direct fission product ^{133}Cs to form ^{134}Cs. The production can hence be approximated as a quadratic function of the burnup.

The quadratic behaviour can be seen in figure 3.10, which shows the buildup for two different enrichments. It can be seen that a higher enrichment causes a smaller production of ^{134}Cs. This behaviour can be explained as follows; to accomplish a given burnup, fewer neutrons are needed for a higher enrichment and fewer neutrons will therefore be available for ^{134}Cs production through absorption in ^{133}Cs.

The mass chain yields are approximately the same for the fissile uranium and plutonium isotopes, and hence the production of ^{134}Cs [15].

Studies on the buildup when different fractions of void are present in the reactor have been done. The average void was simulated to be 44% or 77%. The effect is that for a higher void, which implies less water and thus less moderation, more neutrons with a higher average energy can participate in the formation of ^{134}Cs through the resonance absorption in ^{133}Cs.

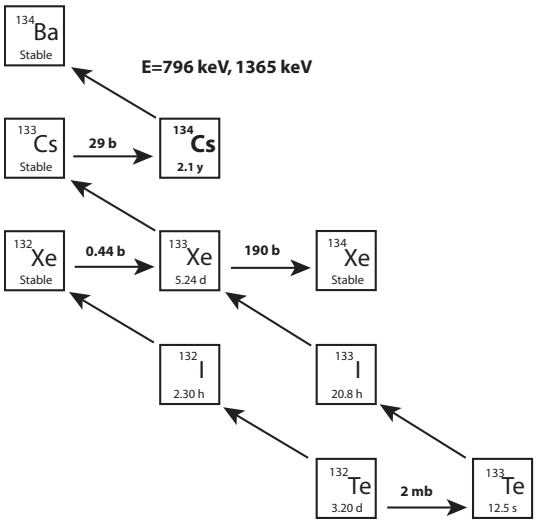

Figure 3.9: The production path of ^{134}Cs. The neutron capture reaction in ^{133}Cs also has a resonance of 421 barns for intermediate neutron energies which is a significant contributor to the production of ^{134}Cs. The most prominent gamma ray energies of ^{134}Cs have been depicted in the figure.

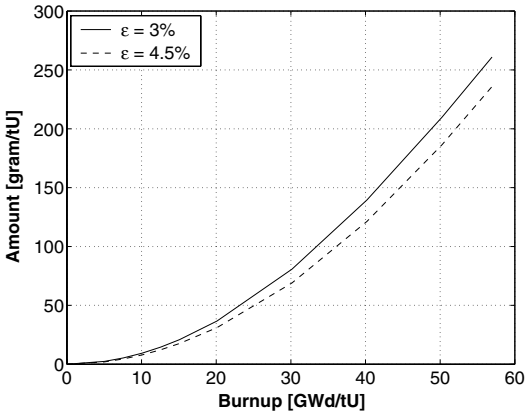

Figure 3.10: The quadratic dependence on burnup for the production of ^{134}Cs. The simulation was performed on a 17 × 17 PWR fuel.

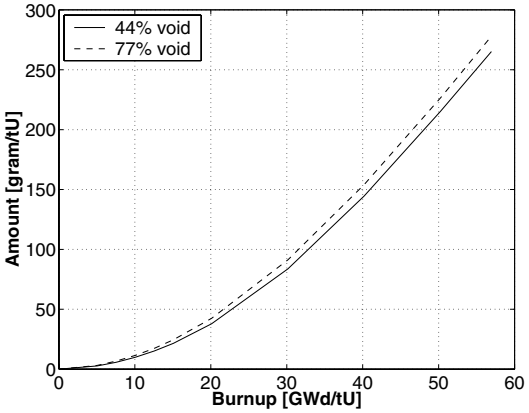

Figure 3.11: The influence of different average void on the production of ^{134}Cs illustrated from simulations of a 7 × 7 BWR fuel assembly.

3.4.5 The production of ^{154}Eu

The production of ^{154}Eu is the most complicated of the three isotopes. It is produced via about 20 different reaction chains [16] and only to a small extent as a direct fission product. The production is governed by a series of β decays and neutron absorptions. As in the case of ^{134}Cs, simulations for different enrichments and voids have been done, these can be seen in figure 3.12 and 3.13. The production can be seen to be a power function of the burnup, but in many cases a quadratic description of the buildup is a good approximation.

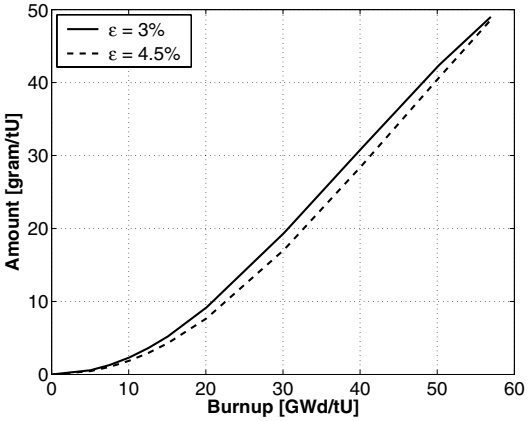

Figure 3.12: The nearly quadratic behaviour of the ^{154}Eu production for two different enrichments.

Also here, higher enrichment has the effect of a lower production of ^{154}Eu. As for ^{134}Cs, higher enrichment requires a lower neutron flux to

accomplish a given burnup and less neutrons are available for capture reactions.

The simulations with different average voids are shown in figure 3.13. For a reactor with higher average void the production of ^{154}Eu is also higher. Less water makes the neutron spectrum shift to being harder (more high energy neutrons) and many resonances in the neutron absorption cross section above thermal energies result in a larger production of ^{154}Eu.

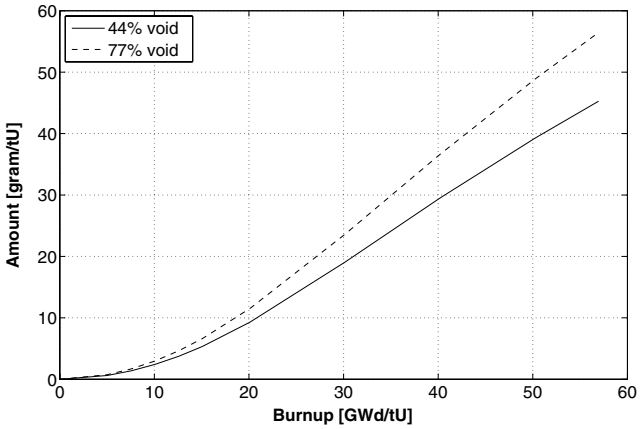

Figure 3.13: The influence of different average void on the production of ^{154}Eu. A 7 × 7 BWR fuel was used in the simulations.

It has been concluded that this element does not migrate, neither radially nor axially in the fuel [15].

Regarding the fission yield, it can be seen [14] that it is quite different for plutonium and uranium. The fission yield from ^{239}Pu is almost 3.5 times larger than the fission yield from ^{235}U. The effect of different yields from uranium and plutonium is utilized in Paper II.

3.5 Decay heat in spent nuclear fuel

After a fuel assembly has been removed from the reactor, the radioactive fission products continue to decay and create heat by particle and electromagnetic radiation absorption in the fuel matrix. As discussed in section 2.4, the decay heat is an important design parameter for the encapsulation of spent nuclear fuel.

The decay heat can be calculated using various computer codes, in figure 3.14 ORIGEN-ARP has been used for a typical 17 × 17 fuel assembly with a burnup of 40 GWd/tU. The decay heat directly at discharge is a few hundred kilowatts but drops rapidly within the first year. After a cooling time of 30 years, the residual power has dropped to a few hundred watts.

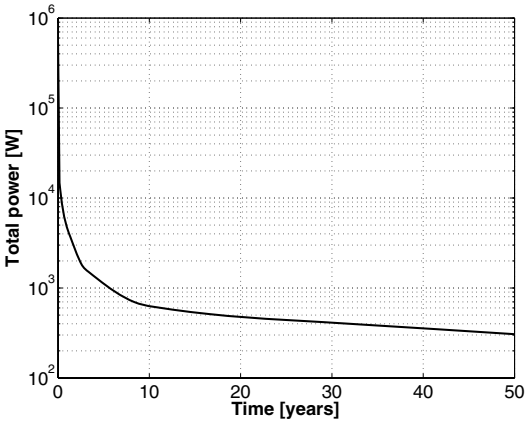

Figure 3.14: The decay heat for a 17×17 assembly with a burnup of 40 GWd/tU. The enrichment was set to 3.1%. The figure represents the decay heat the first 50 years after discharge which can be seen as a typical time the fuel assembly is kept at the interim storage before encapsulation.

The decay heat at this time comes mainly, $\sim$ 60%, from fission products and the remaining 40% comes from heavy elements and actinides. Over time, the actinides increase their relative contribution to the decay heat due to their long half lives. For MOX fuel, the decay heat emanates from a slightly different isotopic composition. The amount of fission products is about the same as for ordinary uranium fuel, but the amount of actinides is higher due to the larger initial amount of actinides in the fuel. The higher actinide content also makes the decay heat higher.

The decay heat calculations of spent nuclear fuel can typically be performed with an accuracy of a few percent [17].

4. The need for measurements

From chapter 1 it is clear that the treaties setup by the IAEA must be experimentally verified by performing safeguards inspections. Presently, a number of different methods are available for different types of safeguards measurements [18]. The methods presented in this thesis have been developed for different safeguards purposes and with the intent to be as robust as possible. An important safeguards task is to verify a State's nuclear inventory and the experimental method used should be stable and accurate in that sense that possible illicit declarations should be detected within the experimental accuracy.

A civilian operator that wants to run a nuclear program for producing plutonium for military purposes must do so in violation with the NPT. For an ordinary LWR, the weapons grade plutonium content is maximized if the reactor is run in short cycles and at a low neutron flux density. In this context though, it should be noted that a more efficient way of producing plutonium would be to use a dedicated reactor for this purpose.

It can be anticipated that an operator that wants to run a reactor for military purposes will declare the fuel assemblies as being part of the ordinary power producing cycle. It is therefore a safeguards interest to verify that the declared irradiation history of a nuclear fuel assembly is compatible with a normal civilian power producing scheme. This specific issue is addressed in section 6.1 and Paper I.

The use of plutonium rich MOX fuel for power production in some reactors makes it a safeguards issue to be able to determine experimentally if a fuel is of MOX type or of the ordinary uranium type. This is also of operator interest at an encapsulation plant for spent nuclear fuel because the higher decay heat in MOX fuel as compared to LEU fuel, makes the temperature limit more difficult to keep for MOX fuel assemblies.

The discrimination of MOX fuel from LEU fuel has been addressed in section 6.1.4 and Paper II and the decay heat determination and verification in section 6.3 and Paper IV.

5. Equipment and analysis

Spent nuclear fuel assemblies emit a flux of particles, such as neutrons, anti neutrinos and gamma rays. Neutrons from the spontaneously fissioning isotopes ^{242}Cm and ^{244}Cm have been used for burnup and fuel completeness measurements, see for instance [19] and [20], and anti neutrinos have been suggested for safeguards purposes [21]. This work has focused on using the emission of gamma radiation to gain knowledge about the fuel assembly.

5.1 Detecting gamma radiation

Gamma rays are emitted from radioactive nuclei in the decay process. A gamma ray has a defined energy and radioactive nuclei emit many gamma rays with, in general, different energies while others only emit one gamma ray with one energy. By measuring the energy of the gamma rays it is possible to deduce from which isotope these are emitted, since the energies are well known for all radioactive nuclei. It is known how ^{137}Cs is produced in the reactor during irradiation as well as the energy of its gamma ray. If we can measure gamma rays with that particular energy, we thereby know that ^{137}Cs must be present in the fuel.

The energy of the gamma rays is measured in *kilo electron volts*, keV[1].

A spent nuclear fuel assembly is a radioactive source of extremely high intensity with a large number of different radioactive nuclei emitting a vast selection of gamma ray energies. This puts a few demands on the detector system which will be accounted for in the coming sections.

5.1.1 Detector system

The great complexity of the gamma ray energy distribution from a spent nuclear fuel demands a detector with suitable characteristics. The most common detector for performing gamma ray spectroscopy with complex energy spectra is the germanium detector, which was also chosen for this work. It is capable of separating closely lying gamma ray energies, i.e. it has a good energy resolution. The relatively high density of germanium implies

[1] An electron that is accelerated over a potential difference of 1 kV will gain a kinetic energy of 1 keV. For instance the energy of the gamma ray emanating in the decay of ^{137}Cs has an energy of 661.657 keV [22].

a good photoelectric absorption but at the same time the small bandgap of germanium requires cooling of the detector. This is done in order to avoid the large thermally induced leakage current that otherwise would occur in the system, making operation impossible at room temperature. The germanium detector is therefore cooled during operation with liquid nitrogen to a temperature of 77 K.

For practical and economical reasons the measurement times should be reasonably short so the detector system should have a high detection efficiency which requires a large detector. Since high gamma ray intensities can be expected, the system should be designed to be able to operate at high counting rates. The germanium detector used had a relative efficiency of ~80% and was equipped with a transistor reset preamplifier. The transistor reset amplifier has a lower noise level and can be operated at a higher rate than traditional charge sensitive preamplifiers.

For the data taking, the detector was connected to a computer with an Aptec-NRC MCArd multi channel analyser with 4096 channels. The MCArd was equipped with three different amplifier types, unipolar, bipolar and gated integrator [23].

A typical energy spectrum from a fuel assembly recorded with a germanium detector is shown in figure 5.1.

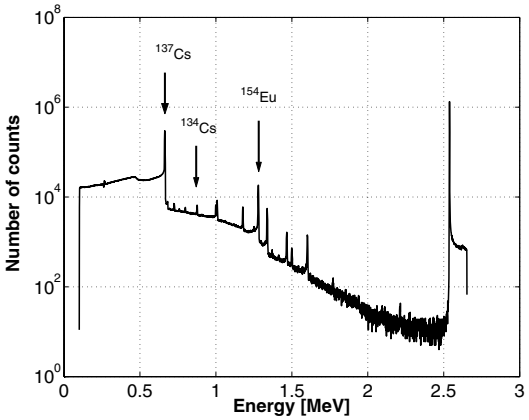

Figure 5.1: A typical energy spectrum from a spent PWR nuclear fuel assembly. The burnup was 47 GWd/tU and the cooling time 12 years.

The three isotopes most prominent in fuel assemblies with a few years cooling time are indicated with their respective names. The large peak on the far right is an artificial pulser peak used for spectrum evaluation, see section 5.1.2. Two of the stronger peaks around ^{154}Eu come from ^{60}Co, which is an activation product. Nickel is a component of structural materials and under neutron radiation this transforms to Cobalt via ^{60}Ni(n,p)^{60}Co. ^{60}Co has two gamma ray energies of 1.17 and 1.33 MeV which are clearly seen.

5.1.2 Dead time correction

A detector system can only handle incoming pulses up to a rate before the pulses arrive so closely that the system has not finished processing one pulse before the next arrives. The minimum time (the dead time) that the system can handle is dependent on both the detector itself as well as the electronics in the collecting system. Any pulse that arrives when the system is processing another one is lost and at high counting rates these losses can be large and it is therefore important to correct for this.

A number of methods can be used for this correction, for the experiments presented in this thesis, the pulser method has been used [24]. This is based on using an electronic pulse generator that injects artificial pulses to the detector system at a well defined rate. In such a way a peak is created in the spectrum, see figure 5.1. It is assumed that the dead time of the artificial pulses is the same as for the gamma events. By forming the ratio between the the pulser rate and the rate registered in the detector system, a correction factor is obtained for which all intensities in the measurement should be multiplied with.

5.2 Mechanical equipment

All Swedish BWR reactors as well as the interim storage CLAB has the installation for fuel measurements depicted in figure 5.2 built in.

A fuel assembly is placed in a movable fixture which is mounted on the pool wall. The fixture can be moved vertically and it is also possible to rotate the fuel around the fuel axis. The vertical speed as well as the rotational speed can be changed.

Built into the pool wall is a collimator which selects the emitted radiation in a well defined direction towards the detector, which is mounted at the back end of the collimator. The collimator can be seen in figure 5.3. The collimator, made of two massive steel half cylinders, allows the radiation from the full diagonal of the fuel assembly to reach the detector. The height of the collimator can be varied between 1, 2 and 3 mm. This height variation is used to adjust the counting rate in the detector.

At the back end of the collimator, a filter of a lead and a copper plate is used to filter out low energy gamma rays that load the detector system with radiation unnecessary for this application[2].

At the beginning of a measurement, the fuel assembly is placed with one of the corners facing the detector as seen in figure 5.3. The accuracy in the positioning of the fuel assembly with respect to the collimator slit is a few millimeters vertically and about 1° angularly. The fuel assembly is then

[2]The lead plate absorbs the undesired gamma rays and the copper plate is used for absorbing the X-rays produced in the lead due to the absorption process.

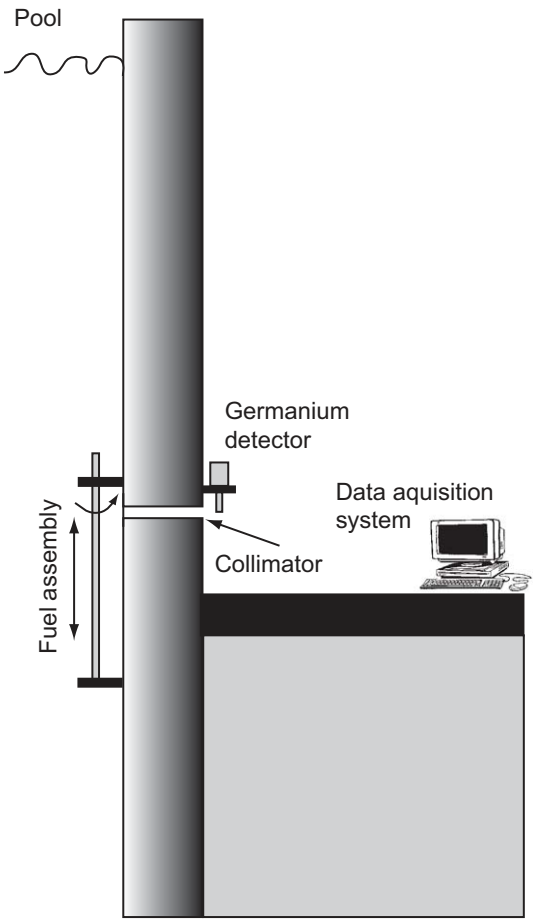

Figure 5.2: The mechanical installation used for performing the measurements. The figure shows the pool and pool wall from the side. The fuel assembly can be moved up and down as well as rotated around its vertical axis.

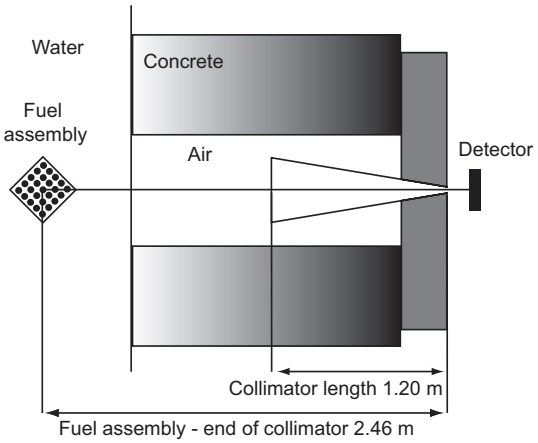

Figure 5.3: As schematic picture of the collimator as seen from above. The triangular shape of the collimator is wide enough to cover the diagonal of the fuel assembly. The height of the collimator can be varied between 1, 2 and 3 mm.

moved vertically in front of the horizontal collimator slit while the detector registers the gamma radiation. When one corner has been scanned, the fuel assembly is rotated 90° and the next corner is scanned in the same manner as the first one. This procedure is repeated for all four corners. The reason for scanning the corners of the fuel is that the positioning error is reasonably small around the corners [25].

It should be noted that this system has been used because it is easy accessible and already installed. It is however not optimized for the experiments presented in this thesis but offers a good platform for testing the methods presented here.

5.3 Data acquisition software

The software for collecting the gamma ray spectrum was written specially for this type of measurements. The used Aptec-NRC MCArd comes with the option of using the signals from the card in software written specially for any application. The program was written to be able to collect spectra during short times.

As the fuel is scanned, the side of the fuel is sampled in about 200 subspectra, each representing a measurement time of about 1 s which corresponds to a fuel length of 2 cm with the scanning speed used in this work. This subdivision of the spectra is done because the counting rate may vary significantly along the length of the fuel assembly and at the same time, an intensity profile of the fuel assembly is obtained. Each subspectrum is corrected for dead time as described in section 5.1.2. When one side of the fuel assembly has been scanned all dead time corrected subspectra are added to

form one spectrum representing one side of the fuel. The four corner spectra are added to one, which then represents the fuel assembly as a whole.

5.4 Data analysis

The evaluation of all subspectra were performed with a software package specially written for this task [26].

The analysis software is an offline tool that is used to perform the analysis of the gamma ray spectra. The program calculates the fuel assembly parameters such as the decay heat by using the ^{137}Cs intensity and the burnup, cooling time and the axial isotope distribution by using ^{137}Cs, ^{134}Cs and ^{154}Eu, see chapter 6 for the details.

The software can be used for either manual or automatic analysis of the gamma ray spectra. In automatic mode, the software performs e.g. peak search and identification, determines peak boundaries, background subtraction and determination of peak area. For the background subtraction, lower and upper baselines of the peak are defined by determining these on either side of the centroid. These baseline regions are used to define the background level to be subtracted from from each channel of the investigated part of the spectrum. The background is defined as a step function below the peak [27]. The evaluation of the peak area was done by summing the intensities in each channel defined as the peak after background subtraction was performed.

Since the intensities of the isotopes are determined for every subspectrum, detailed information of the concentration of these along the fuel axis is obtained. Because the intensity of ^{137}Cs is directly proportional to burnup, the burnup profile of a fuel assembly is thus obtained. An illustration of such a profile is shown in figure 5.4. Each data point represents the ^{137}Cs intensity in one node of the fuel assembly. The measurement time for each data point is here around six seconds which represents about 10 cm of fuel.

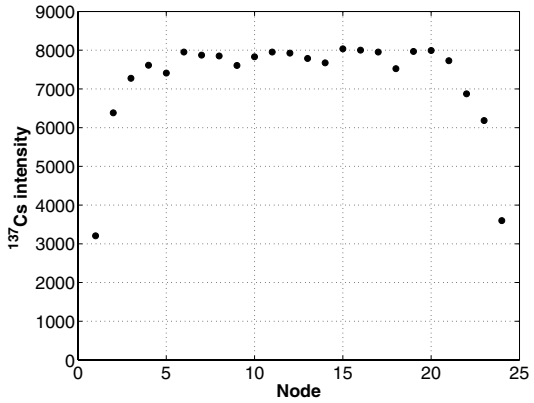

Figure 5.4: The ^{137}Cs intensity along the fuel length. The figure can also be said to represent the burnup profile of the fuel because of the linear relationship between ^{137}Cs and burnup. The recorded spectra have been grouped into 24 nodes, the dips in the intensity distribution are the spacers of the fuel assembly.

6. Methods and applications

The measurement system comprising of the scanning equipment together with the detector and data acquisition as presented in chapter 5 is here referred to as high resolution gamma ray spectroscopy, HRGS. In this thesis, the HRGS method is the common feature of the whole experimental part. The fuel assemblies are scanned the same way and the data collecting is the same, it is also applied in the same way regardless of fuel type (BWR, PWR or MOX) or fuel geometry (8×8, 14×14, 15×15 or 17×17). The data taking and evaluation of the spectra follows the description in chapter 5.

Each measurement campaign requires a normalization of the system. A reference fuel assembly is most easily utilized. This is a fuel assembly that is considered fully known with respect to the fuel assembly data, for instance cooling time, irradiation history (and hence the burnup), enrichment and geometry. In this way, the measured intensities of the isotopes can be related to known fuel data and normalization constant can be obtained.

The calibration constant can be seen to be a product of two factors, $\boldsymbol{A}$ and $\boldsymbol{B}$. The first factor, $\boldsymbol{A}$, depends on the geometry of the fuel assembly and the second factor, $\boldsymbol{B}$, depends on the detector properties and the geometry of the collimator. The gamma ray transport through the fuel matrix is the most important factor of $\boldsymbol{A}$. The second factor, $\boldsymbol{B}$, can in turn be described by the following parts.

- The effective area of the assembly seen from the detector.
- The solid angle covered by the detector as seen from the assembly.
- The transmission of the radiation between the fuel assembly and the detector.
- The intrinsic efficiency of the detector, i.e. the probability that a gamma quanta hitting the detector results in a full energy event in the detector system.

The calibration holds for all fuel assemblies of the same geometry but needs to be reestablished if the detector or measurement setup is altered.

6.1 Irradiation history verification

An important safeguards task is to verify that a given declaration for a specific fuel assembly is the right one. If such a declaration is missing or can be considered untrustworthy, it is still possible to experimentally determine

the burnup and cooling time of a fuel assembly as long as the fuel type (BWR, PWR, MOX) and geometry (15 × 15 for instance) are known.

6.1.1 Semi empiric verification of the fuel parameters

When authorities such as IAEA or Euratom want to verify the correctness of a given fuel assembly declaration a semi empiric verification may be performed. It is semi empiric in the sense that data from gamma scanning is combined with calculated data. In this case, an isotopic content in the spent fuel assembly is calculated using a computer code and related to measurement of the same isotope according to (6.1)

$$i_x \cdot \mathrm{e}^{\lambda_x CT} = K_x \cdot I_x. \tag{6.1}$$

In equation (6.1), i_x represents the measured intensity of the isotope x, $\mathrm{e}^{\lambda_x CT}$ represents the correction factor for cooling time (CT) of the measured isotope, λ_x is the decay constant. The calibration constant is denoted K_x and the calculated isotopic content is denoted I_x. The equation describes what the measured intensity should have been if measured at fuel discharge. This quantity should equal the corresponding calculated isotopic content, multiplied with the calibration constant K_x.

Rearranging (6.1) and solving for CT we get the following expression

$$CT = \frac{1}{\lambda_x} \ln\left(\frac{K_x \cdot I_x}{i_x}\right). \tag{6.2}$$

An easy and simple way to check a declared history is to simulate the declared irradiation history to get I_x for the given fuel assembly. Equation (6.2) is then used to calculate the cooling time. It is advantageous to use ^{134}Cs because of its short half life. If the calculated cooling time agrees with the declared one, this is an indicator of a correct declaration. Especially since the stated irradiation history is explicitly used in calculating the quantity I_x. The deviation from the declared value can be written as

$$\Delta_{134} = CT_{134} - CT_{\mathrm{decl}}. \tag{6.3}$$

If the calculated CT should differ from the declared it is however ambiguous if it is the declared cooling time that is wrong or if the irradiation history is wrongly declared. How can this be decided in such a case?

If the irradiation history is correctly declared, the calculation of CT should give the same answer no matter which isotope is used. In this context, two combinations of the three isotopes have been utilized in the way presented in (6.4)

$$\begin{cases} CT_1 = \frac{1}{\lambda_{137}-\lambda_{134}} \ln\left(\frac{K_{137}\cdot I_{137}\cdot i_{134}}{K_{134}\cdot I_{134}\cdot i_{137}}\right), \\ CT_2 = \frac{1}{\lambda_{154}-\lambda_{134}} \ln\left(\frac{K_{154}\cdot I_{154}\cdot i_{134}}{K_{134}\cdot I_{134}\cdot i_{154}}\right). \end{cases} \tag{6.4}$$

The purpose of this approach is to use the three isotopes which all have different buildup paths in the fuel assembly and a correctly declared irradiation history should then result, in principle, in identical cooling times CT_1 and CT_2.

The difference in CT_1 and CT_2 should be less than

$$|CT_1 - CT_2| < (\Delta CT_1 + \Delta CT_2). \tag{6.5}$$

Here, ΔCT_1 and ΔCT_2 represent the uncertainty of CT_1 and CT_2. It can be noted that equation 6.5 represents the most conservative estimate corresponding to full correlation of the errors in CT_1 and CT_2.

6.1.2 Empiric determination of the fuel parameters

One may foresee cases in the future when information on a fuel assembly is partly or entirely missing. From HRGS data one may experimentally obtain the burnup and cooling time of an assembly even if no declared data is available. The expression in equation (6.6) holds

$$i_x \cdot e^{\lambda_x CT} = C_x \beta^{\kappa_x}. \tag{6.6}$$

In this expression, β represent the discharge burnup and κ, the dependence on burnup, is set to 1 when using ^{137}Cs and set to 2 for ^{134}Cs and ^{154}Eu as described in section 3.4. C_x is here the corresponding calibration constant as in the previous section. Solving (6.6) for β using ^{137}Cs gives

$$\beta = \frac{i_{137} \cdot e^{\lambda_{137} CT}}{C_{137}}. \tag{6.7}$$

Solving (6.6) for β using ^{134}Cs (or ^{154}Eu) where κ is set to 2 yields

$$\beta = \left(\frac{i_{134} \cdot e^{\lambda_{134} CT}}{C_{134}} \right)^{\frac{1}{2}}. \tag{6.8}$$

Combining (6.7) and (6.8) and solving for β and CT results in

$$\beta = \left(\frac{i_{134}}{C_{134}} \left(\frac{C_{137}}{i_{137}} \right)^{\frac{\lambda_{134}}{\lambda_{137}}} \right)^{\frac{\lambda_{137}}{2\lambda_{137} - \lambda_{134}}} \text{ and} \tag{6.9}$$

$$CT = \frac{1}{\lambda_{134} - 2\lambda_{137}} \ln \left(\left(\frac{i_{137}}{C_{137}} \right)^2 \cdot \frac{C_{134}}{i_{134}} \right). \tag{6.10}$$

Any combination of the isotopes can be used but here the combination of ^{137}Cs and ^{134}Cs has been chosen due to the large difference in half life of these two isotopes.

6.1.3 Accuracy of the semi empiric and empiric methods

Two sources of uncertainties must be considered, the experimental uncertainty and the calculated uncertainty. For the fuel assemblies investigated for this purpose, a statistical accuracy of 0.05%, 0.15% and 0.15% for ^{137}Cs, ^{134}Cs and ^{154}Eu was obtained, respectively.

Two computer codes were used for the calculations of the isotopic content, I, ORIGEN-ARP and the Spent Nuclear Fuel code (SNF). According to [28], ORIGEN-ARP calculates I with a standard deviation of 0.5%, 2.2% and 3.2% for ^{137}Cs, ^{134}Cs and ^{154}Eu, respectively. SNF is based on CASMO-4/SIMULATE-3 [29, 30], which are detailed core physics codes, so the accuracy is expected to be the same as or better than ORIGEN-ARP.

With these values it can be seen that the accuracy of (6.2) is 27 days (1σ) when using ^{134}Cs. This implies that a cooling time calculation using (6.2) that lies within around 100 days ($3-4\sigma$) may be regarded as a fuel assembly with a correct declaration.

Using the stated accuracies for (6.4) gives $\Delta CT_1 = 9$ days (1σ) and $\Delta CT_2 = 22$ days (1σ). Equation (6.5) can therefore be rearranged as

$$|CT_1 - CT_2| < 31\text{days}. \tag{6.11}$$

The correlation coefficient is set to 1 due to the correlation between CT_1 and CT_2 and (6.11) is therefore a conservative estimate of the total uncertainty. If the difference in (6.11) is less than 31 days, the fuel may be considered to be correctly declared, provided that equation (6.3) also holds.

For (6.9) and (6.10) it can be shown that an uncertainty of one percent of the measured intensities of ^{137}Cs and ^{134}Cs gives an uncertainty in CT of 28 days. In the same manner, the relative difference of the calculated β is 1.2% for a measured intensity uncertainty of one percent in the two isotopes. However, for fuel assemblies with a cooling time exceeding about 20 years or more, it may be necessary to use the combination ^{137}Cs and ^{154}Eu. The corresponding uncertainty in (6.9) and (6.10) is then 235 days for the cooling time and 2.4% for the burnup assuming the same conditions as previously stated.

6.1.4 Discriminating MOX fuel from LEU fuel

From a safeguards point of view it is of interest to experimentally determine whether a fuel assembly is of MOX type or of LEU type. One reason is the large content of different plutonium isotopes in a spent MOX fuel as compared to LEU fuel. As an example, the isotopic content of two fresh fuel assemblies of the two types can be seen in table 6.1.

After irradiation, the isotopic composition of MOX and LEU differs. The higher plutonium contents in spent MOX fuel, especially the higher ^{238}Pu, ^{241}Pu, americium and curium contents, are by far the largest contributors

Table 6.1: *The isotopic content of fresh MOX and LEU fuel. The MOX fuel content was adapted from [31].*

Isotope	**Weight percent**	
	MOX	LEU
^{238}**Pu**	2.5	–
^{239}**Pu**	54.7	–
^{240}**Pu**	26.1	–
^{241}**Pu**	9.5	–
^{242}**Pu**	7.2	–
^{234}**U**	0.00119	0.0267
^{235}**U**	0.25	3
^{236}**U**	–	0.0138
^{238}**U**	99.74881	96.9595

for making spent fuel management more challenging for MOX than for LEU fuel [32].

The presented method for identifying MOX fuel is based on the fact that ^{134}Cs and ^{154}Eu are produced in very different concentrations in MOX fuel as compared to LEU fuel. As discussed in section 3.4.5, the fission mass chain yield is about a factor of 3.5 times larger for plutonium than for uranium, see table 6.2.

Table 6.2: *The thermal fission mass chain yields of ^{134}Cs and ^{154}Eu as reported in [14].*

Isotope	**Thermal fission mass chain yield (nuclei per 100 fissions)**		
	^{235}**U**	^{239}**Pu**	^{241}**Pu**
^{134}**Cs**	7.87	7.68	7.92
^{154}**Eu**	0.074	0.26	0.38

The impact of these different fission yields were studied with a simulation using ORIGEN-ARP. The MOX fuel was modelled according to table 6.1. The MOX fuel was modelled having a total plutonium content of 4.67% which equals a fissile content of 3.00%. The uranium fuel was mod-

elled having an enrichment of 3.00%. The calculated burnup dependence of ^{154}Eu and ^{134}Cs can be seen in figure 6.1 and 6.2.

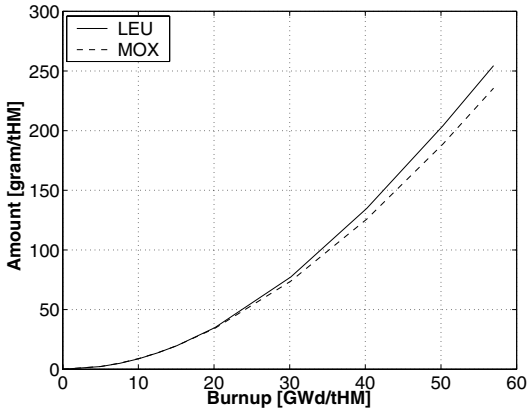

Figure 6.1: Comparison of the content of ^{134}Cs in 3% enriched MOX and LEU fuel as obtained from ORIGEN-ARP, using a five power cycle history.

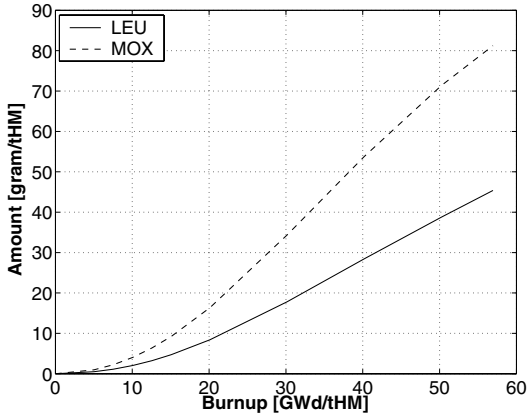

Figure 6.2: Comparison of the content of ^{154}Eu in 3% enriched MOX and LEU fuel as obtained from ORIGEN-ARP, using a five power cycle history.

For ^{134}Cs, the isotope production is slightly lower for MOX fuel than for LEU fuel. This is explained by the fact that the fission and overall absorption cross sections of ^{239}Pu are substantially higher than those of ^{235}U. For the same power level, MOX fuel therefore requires a lower thermal neutron flux.

For ^{154}Eu, the yield in MOX fuel is about a factor of two larger than the LEU fuel. It is smaller than what is inferred from table 6.2, because of the lower flux of thermal neutrons.

Suggested method for discriminating MOX fuel from LEU fuel

From figure 6.1 and 6.2 it is suggested to form the ratio of the ^{134}Cs and ^{154}Eu intensities for the two fuel types. The ratio of these two intensities is robust in the sense that it is not very sensitive to geometry variations of the experimental setup.

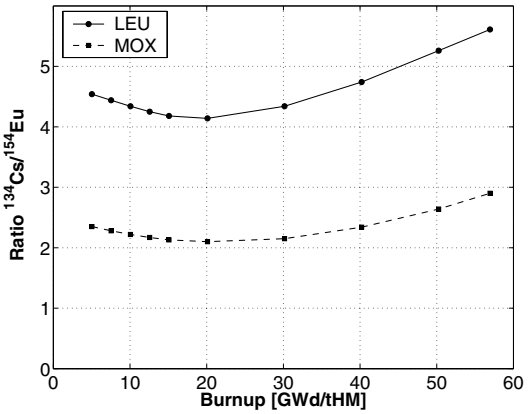

Figure 6.3: The ratio ^{134}Cs/^{154}Eu for fuel with with 3% fissile enrichment. Five consecutive power cycles were simulated.

In figure 6.3, the intensity ratio is shown and as can be seen, the separation is about a factor of two between the MOX and LEU fuel for the whole burnup range of interest here. The dependency on enrichment and irradiation history was also studied which is discussed below.

Since MOX fuel contain more plutonium than LEU fuel a diversion scenario of the MOX fuel for illicit use must be considered. A MOX fuel may be replaced with an LEU fuel assembly to cover the diversion [33]. In order to investigate this case, a calculation was made in which the LEU fuel was assumed to be irradiated for three cycles while the MOX fuel was irradiated for one power cycle. This can be seen as an attempt to replace a plutonium rich MOX fuel with a one cycle burnup with a LEU fuel with a three cycle burnup.

The assemblies were assumed to have the same discharge burnup. As figure 6.4 indicates, the separation between MOX and LEU is somewhat lower but still around a factor of 1.7.

The ^{134}Cs/^{154}Eu ratio has also been simulated for different enrichments. The enrichments were chosen to represent the span most often encountered today in spent nuclear fuel. Also here, the separation of the curves is between 1.6 and 2.4 for the illustrated burnup range.

It is foreseen that this method may be relevant at storage facilities for spent nuclear fuel where both MOX fuel and LEU are kept.

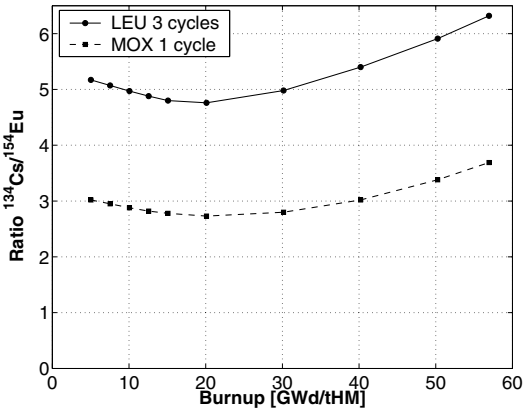

Figure 6.4: The ^{134}Cs/^{154}Eu ratio when different irradiation histories were simulated. The MOX fuel was irradiated for one cycle and the LEU fuel for three cycles.

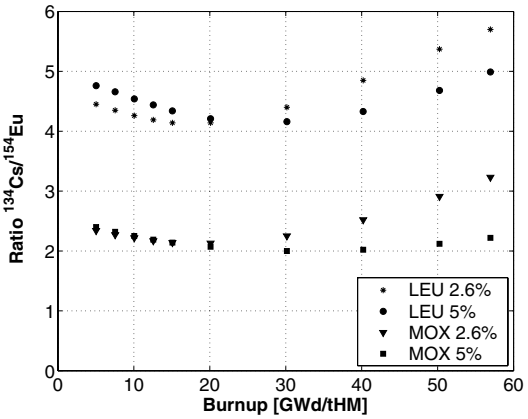

Figure 6.5: The ^{134}Cs/^{154}Eu ratio for different fissile enrichment. Five power cycles were simulated. The separation can be seen to be around a factor of two.

6.2 Improvements of the gamma ray scanning technique

In Paper III, a continuation of the work presented in Paper I has been done. Improvements and suggestions to the measurement strategy has been examined of which a few are addressed here.

At a future encapsulation plant, many fuel assemblies will be verified and determined, with respect to the fuel parameters discussed previously, and a fast measurement method is therefore of key interest. As an improvement for the gamma scanning technique to be faster, it has been proposed to scan the middle part of the fuel assemblies, thereby reducing the measurement time with about a factor of two.

The use of reference assemblies have been further developed. It would be of interest to have as few reference assemblies as possible to minimize the fuel handling. It has therefore been proposed to use only one reference fuel assembly per reactor type (BWR/PWR) because of the different reactor characteristics involved. Additionally, within each reactor type, there is a number of different assembly designs further motivating the use of one reference assembly. The suggested improvement can be accomplished by modelling the reference assemblies, using a suitable computer code, where the radiation contribution from each fuel rod to the detector signal is calculated. From this information normalization factors between the different fuel assembly types can be formed.

Gamma scanning for partial defect studies have also been theoretically investigated. A fuel assembly was modelled with 100 centrally placed fuel rods replaced by inactive dummies. By studying two different gamma ray energies from ^{134}Cs (796 keV and 1365 keV) with different penetrability in the fuel matrix.

The different attenuation of the radiation through the fuel assembly gives rise to relative differences in the measured gamma ray intensities as a function of depth. A suitable parameter for this purpose is the ratio between the intensities of the two energies mentioned.

6.3 Determination and verification of decay heat in spent nuclear fuel

Decay heat can be determined in calorimetric measurement, which are very accurate and have been performed. However, these are very time consuming, one measurement can take days to accomplish and a faster method to establish the decay heat would be of interest. In this thesis, gamma spectroscopic methods have been utilized to determine or, where appropriate, to verify the decay heat of spent nuclear fuel. Using HRGS, the measurement time is reduced to about 20 minutes for one fuel assembly.

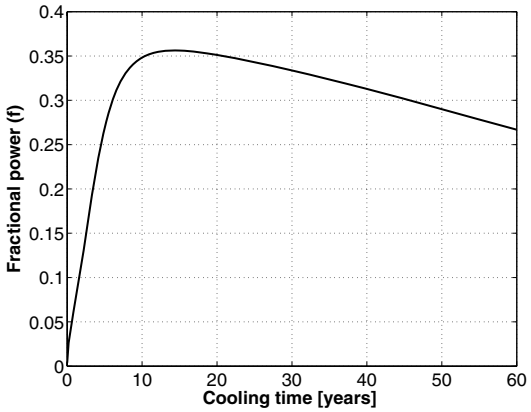

Figure 6.6: The fractional power f as a function of cooling time. The variation is small in the range 15-50 years, the relative variations is decreasing with 0.5%/year.

The method of determining decay heat by measuring the gamma rays in the decay of ^{137}Cs has been described in [20, 34]. A simple relationship exists between the decay heat and the intensity of the gamma radiation from ^{137}Cs, I_{137}. It can be written as in equation (6.12).

$$P = C \cdot \frac{I_{137}}{f} \tag{6.12}$$

The constant C is here a proportionality constant relating a measured ^{137}Cs intensity to the decay heat. The fractional contribution f from ^{137}Cs is defined as

$$f = \frac{P_{137}}{P}, \tag{6.13}$$

where P_{137} is the power developed in the fuel due to the decay of ^{137}Cs.

To illustrate how f depends on the cooling time, figure 6.6 has been calculated using ORIGEN-ARP. As can be seen, the fraction f has a maximum after about 10 years of cooling time. This is because many short lived fission products have decayed by then leaving one of the main contributors to the decay heat to be ^{137}Cs. At the time of the planned encapsulation the fuel assemblies will have a cooling time somewhere around 20 - 50 years, and it is seen in the figure that f has a quite small variation in this cooling time range.

The dependence of f on the initial enrichment and discharge burnup was also investigated. A linear dependence on both parameters could be seen. For the burnup, f decreases with 0.5% per GWd/tU while it increases with 2% per percent unit change of enrichment.

It can be concluded that f does not depend strongly on any of the three parameters with respect taken to the fairly small variation of these fuel parameters for the assemblies subject for final encapsulation. In addition, the

value of f can be estimated based on knowledge of the fuel parameters, as described below.

6.3.1 Decay heat determination

If operator declared data is missing or otherwise questionable so that verification of the decay heat is not achievable or uncertain, it is still possible to determine the decay heat. As seen in figure 6.6, f is relatively constant at the time of encapsulation, which is about 10 - 40 years after f has reached its maximum. An estimation of the burnup and cooling time as described in section 6.1.2 will yield an f value with relatively high precision. In this procedure, the empirically determined values of burnup and cooling time are inserted into a parametrization that represents the fractional contribution f, see equation (6.14).

$$f_{param} = A_0 + A_1 BU + A_2 CT + A_3 CT^2 \tag{6.14}$$

The constants A_0, A_1, A_2 and A_3 are specific to the fuel type studied and can be calculated using e.g. ORIGEN-ARP by evaluating P and P_{137} and thereby obtaining f.

6.3.2 Decay heat verification

If all information is supplied with the fuel assembly, it is easy to feed this information into a computer code such as SNF to calculate the decay heat. However, it is of interest to verify the calculated decay heat experimentally. Since operator declared data is available in this case, the declared burnup and cooling time can be verified as described in Paper I. If these parameters can be considered verified, the burnup and cooling time are inserted into (6.14) to obtain a value of f. This f is then used in combination with the ^{137}Cs intensity to experimentally determine the decay heat. If the determined decay heat and the declared decay heat agree, the decay heat can be considered verified.

This approach is a quick check to verify that the operator declared data is correct by measuring the ^{137}Cs content.

7. Results

7.1 Nondestructive assay of spent nuclear fuel with gamma ray spectroscopy

The methods presented in section 6.1.1 have been tried both on computer simulations as well as on real experimental data. In the simulations, a number of possible irradiation histories were assumed and the method was applied to these irradiation histories. A reference fuel was modelled using ORIGEN-ARP, in this case, a PWR 17×17 fuel assembly with an irradiation history of six power cycles, each 335 days long including a shutdown period of 30 days between each period of irradiation. The burnup was set to 5 GWd/tU per cycle resulting in a discharge burnup of 30 GWd/tU.

Each simulated scenario was then assumed to be reported instead of the actual irradiation history of the reference assembly. A simulated cooling time of ten years (3650 days) was used for all cases.

7.1.1 Erroneously declared discharge burnup

For the first scenario, it was assumed that the operator erroneously declared the fuel data for another fuel assembly than the one being measured. The declared data was reported to be 5.5 GWd/tU per cycle instead of the actual 5 GWd/tU per cycle. The discharge burnup was therefore 33 GWd/tU rather than the reported 30 GWd/tU.

From table 7.1 it is seen that the deviation of CT_{134} from the simulated cooling time, Δ_{134}, is about 200 days, which is in the order of 7 standard deviations from expected. Thus Δ_{134} indicates a clear mismatch between declared and actual fuel parameters. To be able to judge whether the cooling time or the irradiation history is erroneously declared, the difference $|CT_1 - CT_2|$ was calculated. As shown in table 7.1, the value obtained is almost 3 times larger than the standard deviation of 31 days. Taking that as a significant deviation one may conclude that the irradiation history was erroneously declared in this case.

Table 7.1: *Values of Δ_{134} and CT_1 and CT_2, as defined in section 6.1.1, obtained in simulations where the actual burnup per power cycle is 5.5 GWd/tU instead of the reference case of 5 GWd/tU. The values should be compared to the experimental accuracies of 27 days and 31 days for Δ_{134} and for the difference in CT_1 and CT_2, 1σ respectively. The simulated cooling time was 3650 days.*

CT_x	**Cooling time [days]**
CT_{134}	3449
CT_1	3546
CT_2	3627
Δ_{134}	**-201 days**
$\lvert CT_1 - CT_2 \rvert$	**81 days**

7.1.2 Erroneously declared number of cycles

In a second scenario, two alternative irradiation histories were simulated, each resulting in the same discharge burnup as the reference case. These were compared to the reference irradiation history, see table 7.2.

In table 7.2, the reference irradiation history is denoted Fuel_{ref} while the two alternative irradiation histories are denoted $\text{Fuel}_{\text{alt1}}$ and $\text{Fuel}_{\text{alt2}}$. The declared and actual discharge burnup was considered to be equal.

It can be seen that Δ_{134} is about 3 and 6 standard deviations from expected, respectively. However, if (6.4) is applied to these cases the difference in $|CT_1 - CT_2|$ is 18 days and 37 days, respectively. These two cases thus represent scenarios that can be detected but where the conclusion whether the irradiation history or the cooling time is not correctly declared, is dubious.

For the third scenario, shown in table 7.3, two real cases of irradiation histories have been simulated. One assembly has been irradiated for five power cycles, which is considered here to be the declared history, $\text{Fuel}_{\text{decl}}$. The other fuel assembly, Fuel_{alt}, has been irradiated for four power cycles and is here assumed to have been exchanged with the declared fuel assembly.

The deviation Δ_{134} is 193 days, which is about 7 standard deviations from expected. It thus represents clear evidence that the fuel assembly is not correctly declared. However, also in this case it can be seen that the difference $|CT_1 - CT_2|$=17 is below the stated detection limit of 31 days.

7.1.3 Nondeclared outtake

The last scenario that was simulated, represents a case where the fuel assembly was taken out of the core before the last power cycle, left out for 1 –

Table 7.2: *Three different irradiation histories resulting in the same discharge burnup quoted in GWd/tU. $Fuel_{ref}$ is the reference history and $Fuel_{alt1}$ and $Fuel_{alt2}$ are the two alternative histories. The simulated cooling times in each case was 3650 days.*

Cycle	**Fuel**$_{\text{ref}}$	**Fuel**$_{\text{alt1}}$	**Fuel**$_{\text{alt2}}$
	Burnup [GWd/tU]		
1	5	–	–
2	5	6	–
3	5	6	7.5
4	5	6	7.5
5	5	6	7.5
6	5	6	7.5
Σ_{Burnup}	**30**	**30**	**30**
CT_{134}	–	3569	3483
CT_1	–	3576	3498
CT_2	–	3557	3461
Δ_{134}	–	**-81 days**	**-167 days**
$\lvert CT_1 - CT_2 \rvert$	–	**19 days**	**37 days**

5 years and eventually put back in for another irradiation cycle. The burnup for each irradiation cycle was 5 GWd/tU, see table 7.4. These irradiation histories were compared to the reference irradiation history. Also in this case, Δ_{134} and the time difference $|CT_1 - CT_2|$ were calculated as displayed in table 7.4.

Using Δ_{134}, five scenarios are revealed. By using the difference $|CT_1 - CT_2|$, it is seen in table 7.4 that a nondeclared outtake of two years or more results in conclusive information that the irradiation history was erroneously declared.

7.1.4 Experimental results from scanned nuclear fuel assemblies

The experimental study was performed on twelve fuel PWR 17 × 17 assemblies coming from the Swedish nuclear power plant Ringhals 3. The assemblies were evaluated with respect to the count rates of ^{137}Cs, ^{134}Cs and ^{154}Eu.

Table 7.3: *Two real-case irradiation histories with the acquired burnup per cycle. Here it is assumed that these two fuel assemblies have been exchanged so that the declared irradiation history is not correct, although the discharge burnup is similar. It can be noted that the experimental parameter Δ_{134} clearly indicates the erroneous declaration.*

Cycle	**Fuel**$_{\text{decl}}$	**Fuel**$_{\text{alt}}$
	Burnup [GWd/tU]	
1	6.89	–
2	10.42	10.27
3	7.87	10.04
4	6.94	7.62
5	3.34	7.71
Σ_{Burnup}	**35.46**	**35.64**
CT_{134}	–	3457
CT_1	–	3466
CT_2	–	3449
Δ_{134}	–	**-193 days**
$\lvert CT_1 - CT_2 \rvert$	–	**17 days**

No particular reference assembly was assigned for this study, it was assumed that the whole data set could make up the reference. Accordingly, the calibration constants, K_x for the case with available operator-declared data and C_x for the case with no operator-declared data, were determined as an average of the complete data set.

Verification of spent nuclear fuel assemblies with operator declared irradiation histories

For this case, the data from the assemblies were evaluated according to (6.2) and (6.4). The differences $|CT_1 - CT_2|$ and Δ_{134} were calculated and evaluated as described in section 6.1.1. The results can be seen in table 7.5.

As table 7.5 shows, neither $|CT_1 - CT_2|$ nor Δ_{134} indicate any errors in the declaration of the fuel assemblies.

Table 7.4: *Each row represents an alternative irradiation history where the fuel assembly has been out of core for 1 – 5 years before the last irradiation cycle. For each case, the calculated values of* Δ_{134} *and* $|CT_1 - CT_2|$ *are presented.*

Out of core [**years**]	CT_{134} [**days**]	CT_1 [**days**]	CT_2 [**days**]	Δ_{134} [**days**]	$\lvert CT_1 - CT_2 \rvert$ [**days**]
1	3806	3797	3829	156	33
2	3946	3925	3988	296	63
3	4059	4024	4112	409	88
4	4146	4096	4204	496	108
5	4213	4146	4271	563	125

Determination of burnup and cooling time for fuel assemblies where the irradiation history is considered unknown

The case where no operator declared information is available can be treated according to the discussion in section 6.1.1. It can be noted that the discussion requires that the type of fuel assembly may be identified.

The experimentally determined burnup and cooling time are summarized in tables 7.6 and 7.7.

From the values given in table 7.6 it is inferred that the burnup can be determined with a relative uncertainty of 1.6% when using the combination of the ^{137}Cs and ^{134}Cs intensities. Using the combination of the ^{137}Cs and ^{154}Eu intensities yields a relative standard deviation of 4.6%. The corresponding relative uncertainties of the determined cooling times are 1.5% and 15.5%, respectively, as shown in table 7.7.

7.2 Discriminating MOX fuel from LEU fuel for safeguards purposes

The method for discriminating MOX fuel from LEU fuel described in section 6.1.4 has been applied experimentally on 29 PWR fuel assemblies and 9 MOX fuel assemblies. The PWR assemblies were of both 17×17 and 15×15 geometry. The two PWR data sets were irradiated at the Swedish nuclear power plant Ringhals and the MOX fuel assemblies all came from the German nuclear power plant in Obrigheim. The MOX assemblies were of PWR 14×14 geometry. The characteristics of the three fuel types are presented in table 7.8.

All fuel assemblies were measured using the HRGS equipment at the interim storage CLAB and evaluated with respect to the intensities of ^{134}Cs and ^{154}Eu. The ratio ^{134}Cs/^{154}Eu was calculated for the three different fuel geometries and the result can be seen in figure 7.1.

Table 7.5: *The experimental results obtained according to the equations described in section 6.1.1.*

Fuel Id	**Declared** T **[days]**	CT_{134} **[days]**	CT_1 **[days]**	CT_2 **[days]**	Δ_{134} **[days]**	$\lvert CT_1 - CT_2 \rvert$ **[days]**
0C9	3968	3980	3976	3961	12	15
1C2	3972	3990	3974	4004	18	30
1C5	3967	3961	3965	3943	-6	22
2C2	3968	3972	3966	3965	4	1
3C1	3968	3971	3968	3970	3	2
3C5	3968	3951	3957	3943	-17	14
3C9	3968	3967	3967	3958	-1	9
4C4	3972	3966	3956	3987	-6	31
4C7	3968	3951	3967	3940	-17	27
0E2	3196	3181	3216	3182	-15	34
0E6	3198	3206	3200	3220	8	20
1E5	3196	3213	3197	3233	17	36

In figure 7.1, the two theoretical curves described in section 6.1.4 have also been plotted. The curve for the LEU fuel was normalized to the fuel assemblies by locating it to the mean of the assemblies. The position of the curve corresponding to the MOX assemblies, on the other hand, was determined by using the expected separation from the LEU assemblies as calculated with ORIGEN-ARP.

The fact that this curve is located almost exactly on the same position as if it was normalized to the experimental MOX data gives an indication of the validity of the calculations. This, in turn, offers an additional rigidity to the conclusions drawn in the theoretical part of this work regarding the feasibility of the method.

The MOX fuel assemblies are separated from the LEU assemblies with a factor of 1.85 on the average. The separation factor is 1.3 for the closest values and almost 3 for the values most far apart. The data thus shows a clear difference between the two fuel types.

Four assemblies deviate significantly from the expected ratio as simulated with ORIGEN-ARP, two MOX assemblies and two 15×15 LEU assemblies. These are marked with arrows in the figure. The LEU assemblies are not expected to deviate according to the declared information and it still remains to resolve this discrepancy.

Considering the deviating MOX fuel assemblies, these two assemblies were removed from the core for five and six years, respectively, before being

Table 7.6: *Calculated burnup using the two combinations of ^{137}Cs+^{134}Cs and ^{137}Cs+^{154}Eu. Also shown are the deviations from declared burnup.*

Fuel Id	**Calculated β ^{137}Cs + ^{134}Cs [GWd/tU]**	**Deviation from declared burnup [GWd/tU]**	**Calculated β ^{137}Cs + ^{154}Eu [GWd/tU]**	**Deviation from declared burnup [GWd/tU]**
0C9	38.19	-0.46	38.48	-0.17
1C2	32.82	-0.56	31.47	-1.91
1C5	38.56	-0.10	39.17	0.51
2C2	36.32	-0.29	36.13	-0.48
3C1	36.41	-0.29	36.18	-0.52
3C5	38.61	0.06	39.12	0.57
3C9	36.56	-0.04	36.64	0.01
4C4	33.02	-0.37	31.74	-1.65
4C7	38.93	0.37	39.87	1.32
0E2	43.52	1.85	46.17	5.04
0E6	36.18	0.18	35.89	-0.11
1E5	34.56	-0.01	33.65	-0.92
Relative standard deviation		**1.6%**		**4.6%**

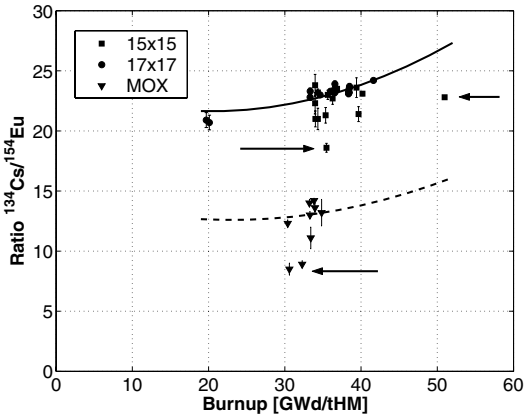

Figure 7.1: The ratio of ^{134}Cs/^{154}Eu as a function of burnup for all fuel assemblies studied in Paper II. The corresponding theoretical values, as calculated with ORIGEN-ARP, have been normalized to the experimental data of the LEU fuel. Two MOX and two 15x15 LEU fuel assemblies deviate significantly from the other, these are marked with arrows. Both the experimental and theoretical data are corrected for decay to the time of discharge.

Table 7.7: *Calculated cooling time using the two combinations of ^{137}Cs+^{134}Cs and ^{137}Cs+^{154}Eu. Also shown are the deviations from declared cooling time.*

Fuel Id	**Calculated CT ^{137}Cs + ^{134}Cs [days]**	**Deviation from declared CT [days]**	**Calculated CT ^{137}Cs + ^{154}Eu [days]**	**Deviation from declared CT [days]**
0C9	3987	19	4106	138
1C2	3905	-67	3237	-735
1C5	3986	19	4237	270
2C2	3952	-16	3867	-101
3C1	3954	-14	3854	-114
3C5	3982	14	4193	-225
3C9	3960	-8	3995	-27
4C4	3895	-77	3267	-705
4C7	4002	34	4382	414
0E2	3327	131	4453	1257
0E6	3197	-1	3067	-131
1E5	3164	-32	2739	-457
Relative standard deviation		**1.5%**		**15.5%**

Table 7.8: *Some of the properties of the three different types of fuel assemblies studied in the experimental part of this work.*

Fuel type	**Enrichment [%]**	**Power cycles**	**Burnup [GWd/tHM]**	**Cooling time [years]**
PWR LEU				
17x17	3.1	2 – 4	20 – 38	14 – 19
15x15	3.2	3 – 5	34 – 51	15 – 21
PWR MOX				
14x14	3.4 – 3.5	3	31 – 35	19 – 24

irradiated for an additional power cycle. During the time out of core, mainly the short-lived ^{134}Cs decays significantly but also ^{154}Eu.

As seen in figure 3.9, the ^{134}Cs is produced from neutron capture in the stable isotope ^{133}Cs. A fuel assembly that is removed from the core and then put back in again will produce relatively much ^{134}Cs due to the amount of ^{133}Cs that is already formed in previous cycles.

Three of the MOX fuel assemblies were also taken out of the core, but after the first irradiation cycle and then put back in again. These were then irradiated for two additional power cycles making the isotopic contents to be almost normal with respect to the level of burnup, i.e. they can not be seen to deviate in figure 7.1.

The relative standard deviation between the experimental and theoretical data was calculated to be 5%, 5% and 8%, respectively for the three fuel geometries 15 × 15, 17 × 17 and 14 × 14, omitting the four deviating assemblies. Taking these assemblies into account, the standard deviation increases to 6%, 5% and 18% for 15 × 15, 17 × 17 and 14 × 14, respectively. The MOX assemblies exhibit the highest standard deviation. A possible reason is the highly irregular irradiation histories.

As a general remark, the declared burnup has in this work been used as a parameter for illustrating the various dependencies of the ^{134}Cs/^{154}Eu ratio. If this parameter, for some reason, is not available, the measured ^{137}Cs intensity can readily be used due to its linear dependency on burnup and weak dependency on all other fuel parameters including irradiation history.

As a complement to the work presented in this thesis, similar theoretical calculations were also performed for BWR fuel. For these calculations it was concluded that the separation of the ^{134}Cs/^{154}Eu ratio was, on the average, a factor of 2, i.e. the method should be feasible also for BWR fuel.

7.3 Improvements of the gamma ray scanning technique

For paper III, a number of measurement improvements were suggested and here two of these are reported, the fuel parameter evaluation of part length measurements and the theoretical investigation of detecting partial defect with HRGS.

The analysis regarding determination of burnup and cooling time as presented in section 6.1.2 has been performed using part length measurements of the fuel assemblies. In table 7.9, such an analysis can be seen, together with deviations from full length measurements, which can be seen as a norm in this context.

The difference between a part length scanning as compared to a full length scanning can in table 7.9 be seen to be small and part length

Table 7.9: *The experimentally determined burnup and cooling time when the middle axial region of the fuel was scanned as compared to when the full length of the fuel assembly was scanned.*

Fuel Id	**Burnup [GWd/tU]**	**Deviation from full length**	**Cooling time [days]**	**Deviation from full length**
4C7	39.0	-0.2	6149	4
4C4	33.5	0.0	6032	13
3C5	38.5	0.0	6128	10
3C1	36.3	0.1	6080	-2
2C2	36.0	0.1	6073	16
1E5	34.6	0.0	5305	0
1C5	38.6	-0.2	6144	1
1C2	32.5	0.0	6055	9
0E6	35.6	0.2	5292	21
0E2	42.9	0.3	5435	6
0C9	38.1	0.1	6117	19
3C9	36.3	0.2	6064	26

Table 7.10: *The ratio between the calculated 796 keV and 1365 keV intensities from ^{134}Cs corresponding to an intact fuel assembly and tampered scenario where 100 centrally located fuel rods have been replaced with dummies.*

Fuel	**796 keV**	**1365 keV**
Intact	1.26	6.82
Tampered	1.13	5.47

measurements can be seen as a simple way of reducing the measurement time.

A theoretical case where a 15×15 fuel assembly was modelled to have its 100 most centrally located fuel rods replaced with dummies, was also performed. The procedure for calculating the intensities as described in Paper III was applied to a fuel assembly with a regular rod configuration as well as to the partial defect case as can be seen in table 7.10.

From table 7.10 the ratio I_{796}/I_{1365} was calculated to be 0.18 and 0.21 for an intact and a tampered fuel assembly, respectively. The relative difference between these ratios of 14% lies well beyond a typical measuring accuracy of about 2 % i.e. this particular partial defect case would yield a result well beyond expected.

7.4 Decay heat

For the decay heat, both experimental verification and determination have been done. Verification for the case where operator data is available and a determination of the decay heat assuming that no operator data is available. 15 PWR 17 × 17 and 16 PWR 15 × 15 fuel assemblies were used in the decay heat measurements.

7.4.1 Verification of decay heat

For the case of verification of the decay heat, the operator declared data is considered available. The relevant data is declared decay heat but inherent in this calculation is the burnup and cooling time. The task is now to verify that the declared decay heat is correct, for which the following steps have been adopted.

1. The operator declared data is verified using the method presented in Paper I. If the declared fuel parameters are considered correctly declared, the declared burnup and cooling time are inserted into equation (6.14) to get an independent value of the fractional power f.
2. The total power is calculated using (6.12) and compared to the decay heat as declared by the operator.

This approach can be seen as an independent verification of the declared decay heat since (6.14) is determined independently of the operator declared data. The parameters A_n were determined by simulating a data set of assemblies with varying fuel parameters using ORIGEN-ARP. The decay heat verification was performed as described and is presented in table 7.11

7.4.2 Determination of decay heat

If operator data is unavailable the decay heat is determined by first determining the cooling times and burnup for the investigated fuel assembly as described in section 6.1.2. For each fuel assembly the fractional power f according to (6.14) was calculated using the constants A_n and the determined values of cooling time and burnup. Together with the calibration constant of (6.12) the decay heat P was calculated. The result of the decay heat determination can be seen in table 7.12 together with the decay heat obtained through calorimetry.

Table 7.11: *The results of the decay heat verification. The standard deviation of the relative difference between the gamma ray measurements and the calorimetric measurements is 2.0%. The table is divided by a horizontal line,* 17 × 17 *assemblies above and* 15 × 15 *assemblies below.*

Fuel Id	**Decay heat gamma scanning [W]**	**Relative difference from calorimetric decay heat [%]**	**Relative difference from calculated decay heat [%]**
3C5	502.07	-0.13	-1.31
0C9	497.58	-1.30	-0.39
2A5	225.45	3.56	5.38
5A3	229.54	2.66	1.70
1C2	417.07	0.14	1.09
1C5	499.92	-0.15	-1.07
2C2	467.30	-0.16	0.49
3C1	472.82	-0.55	-0.62
3C4	500.86	-0.71	-1.38
3C9	471.30	-0.61	-0.34
4C4	429.61	-1.79	-1.92
4C7	505.16	-1.29	-2.07
0E2	588.30	-0.07	-1.60
0E6	480.79	1.43	0.74
1E5	461.42	1.57	0.73
I24	414.85	-1.17	-3.60
I09	509.37	-0.28	0.37
C01	401.78	3.36	3.82
C12	399.06	2.75	3.60
D27	461.51	-1.20	-2.58
F25	392.24	1.14	0.24
D38	450.22	-1.78	-2.46
E38	385.18	-2.63	-3.40
E40	378.22	0.79	-0.73
F14	380.28	0.40	-0.84
F21	415.32	1.33	-0.45
F32	657.92	4.92	4.35
G11	412.28	0.98	-1.27
G23	436.81	-3.85	-5.30
I20	406.97	-0.87	-2.54
I25	462.57	-3.76	-3.20

Table 7.12: *The decay heat measured via gamma scanning independently of operator declared data. The two last columns display the decay heat as measured with calorimetry and the difference between gamma scanning and calorimetry. The table is divided by a horizontal line,* 17×17 *assemblies above and* 15×15 *assemblies below.*

Fuel Id	**Decay heat determined [W]**	**Decay heat calorimetry [W]**	**Relative difference [%]**
3C5	501.79	501.41	-0.08
0C9	496.49	491.17	-1.08
2A5	223.52	233.76	4.38
5A3	225.28	230.25	2.16
1C2	414.58	417.67	0.68
1C5	499.31	499.17	-0.03
2C2	465.65	466.53	0.19
3C1	471.80	470.23	-0.33
3C4	500.47	497.34	-0.63
3C9	470.53	468.42	-0.45
4C4	429.05	422.04	-1.66
4C7	505.78	498.75	-1.41
0E2	592.10	587.90	-0.71
0E6	479.67	487.75	1.66
1E5	460.37	468.77	1.79
I24	414.46	410.07	-1.07
I09	509.32	507.94	-0.27
C01	398.13	415.75	4.24
C12	394.97	410.34	3.75
D27	463.07	456.05	-1.54
F25	390.17	396.75	1.66
D38	449.35	442.34	-1.59
E38	387.41	374.33	-3.50
E40	377.27	381.25	1.04
F14	379.49	381.81	0.61
F21	413.62	420.90	1.73
F32	657.57	691.99	4.97
G11	412.52	416.37	0.92
G23	438.94	420.63	-4.35
I20	405.64	403.46	-0.54
I25	463.31	445.79	-3.93

8. Conclusions and outlook

This thesis describes new ideas to the world of safeguards regarding both verification of operator declared data and determination of fuel parameters in the case where operator data is missing. As the energy debate and the suggested peak-oil theory [35] has gained focus, nuclear energy may be a solution to fulfil the world's predicted energy need in the future. New reactor designs are under construction and with the introduction of these, safeguards will continue to maintain its role as being an important safety barrier. As the new reactor designs are implemented into society, new safeguards need to be introduced and a continuing safeguards research is essential and necessary.

Safeguards will also play an important part in future final repositories, where the safeguards system will face new challenges. For the Swedish system, the long storage time and the fact that the assemblies will not be accessed once they are placed in the repository, are subjects that need to be addressed by safeguards.

All fuel assemblies will be examined before encapsulation. A safeguards issue may arise for assemblies that display measurement results that are inconsistent with declared information. Is a measurement of the decay heat the only parameter that will be crucial if the other safeguards parameters will deviate or will a combination of many parameters need to be correct for a fuel assembly to be considered acceptable?

The HRGS method as presented here is based on existing equipment already installed for other purposes than the suggested methods in this thesis. It is however not dependent or developed for this particular equipment. It may therefore be improved with respect to e.g. measurement geometry, fuel handling and measurement time as well as measurement strategy for optimal conditions serving these strategies. An alternative experimental platform has previously been presented in [36] which allows the detector to be positioned close to the fuel assembly.

For the final storage, a reliable method to determine and/or verify the decay heat is necessary, but also to determine the amount of fissile material present in the fuel assembly. As an outlook for the decay heat verification and determination method presented in Paper IV, a more detailed modelling of the parameter for the fractional power, f, can be done. This would probably result in an increase of the accuracy.

HRGS will probably play a main part in the measurement system of the final storage but it should also be investigated how accuracy and security could be further developed. For these reasons it can be anticipated that gamma ray tomography and neutron measurements will be important. Gamma ray tomography could for instance be used to nondestructively verify the integrity of a fuel assembly as shown in [37] or [38]. A general safeguards approach for the fuel handling with respect to the encapsulation and final storage can be found in [39].

One alternative measurement strategy suggested in this thesis is part length measurement of the fuel assembly. Only the middle part of the fuel assembly is scanned implying a shorter measurement time, but still maintaining a reasonable statistical uncertainty. The results were concluded to only slightly differ from measurements where the full length of the assembly was measured and evaluated. It should be noted that also this experiment could be improved with an alternative or improved experimental setup.

To improve the measurement efficiency, an idea would be to scan the fuel assembly in a spiral manner, i.e. as the spent fuel assembly is moved vertically it can also be set spinning. By using this strategy, the fuel is examined from all sides but only moving the fuel in one vertical direction.

Acknowledgements

What, is this it now? If you read this it means I must have finished and the thesis has been printed. If this is actually the case, a lot of people should be thanked so here goes.

I'd like to start with the man who hired me as a Ph.D. student in the first place, my supervisor Ane Håkansson. One of my first memories is when we visited the reactor hall at Forsmark in 2001 and forgot to put on overalls so we started walking towards the reactor hall in almost nothing but our underwear and shoes before someone found out what was about to happen...Big thanks for the guidance and support these past five years. Anders Bäcklin has also helped in many ways, thank you for your knowledge and ideas which you have shared.

Staffan has helped in many ways, always with a broad and clear vision on how to do things. You also managed to answer my $\sim 10^4$ questions when I did the "En Svensk Klassiker", well done. Accordingly, thank you Staffan.

My office mate Otas and I have always had a great atmosphere in the office during the years, listening to rock, country, reggae and all sorts of music and memorizing African capitals (or, mostly me maybe...). The rest of the present and former members of the Applied Nuclear Physics group, Tobbe, Anni, Ingvar, Marcus, Peter, Pernilla and Karin have made the time here valuable and fun. Mattias Lantz (together with me and Staffan) was involved in breaking out from Imperial College in London in the middle of the night when we attended a course there in 2002, thanks for the help with that and everything else. Robelius Fredrik has shared my recent interest in country music and a lot of other crazy stuff. Good or bad, I now also know more cool guitar moves for which you should be held responsible.

Joa and I found a common interest in cross country skiing the last winters discussing what gliders to use and how bad it hurts when you fall.

The coffee drinking team at the department have made the coffee breaks fun and entertaining so keep up the the good work Örjan, Sophie, Henrik P, Henrik J, David, Emma, Bjarte, Richard and Bengt.

Inger Ericson and Annica Elm are responsible for keeping the department afloat and Ib Koersner and Theresa Kupsc for the computer system. Teddy Thörnlund helped with taking pictures as well as the one for my drivers' license.

The department band of which I have been a part of, **Ib-Karinz**, should of course not be forgotten, Tord J, Kjell, Ib, Karin×2, Henrik, Johan, Ane and

Fredrik. Keep up the good music production for the Christmas parties at the department.

From INF I had the pleasure to get to know Anders, Luca, Henrik, Bumpen, Michael, Philippe, Angelica, Göran and Stephan.

My friends outside the department like Wivis, Sara, Sörensen, Jaana, Mårten, Anna, Erik, Camilla, Lotta, Sacha (joddel joddel), Jeppe, Lena, Jonte, Sofia, Stefan, Catrin, Carl, Matilda are all remembered.

The Swedish Nuclear Power Inspectorate, SKI, has been kind enough to finance my years here and the graduate school for Advanced Instrumentation and Measurements, AIM, has provided means for travelling and interesting courses.

My family deserves a great deal of gratitude, Ann-Christine, Jan and my brother Sebastian. My somewhat crazy ideas about working with nuclear physics have always been encouraged. Thank you Milena for supporting me all years with your never ending enthusiasm and laughter.

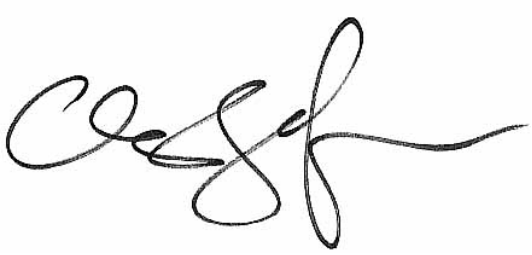

Svensk sammanfattning
Tillämpningar av gammaspektroskopi för kärnämneskontroll

Denna avhandling behandlar mätmetoder för att kontrollera innehållet i använt kärnbränsle. Metoderna kan bland annat användas för att säkerställa att använda bränslen inte används för annat än fredliga syften. De avtal som ligger till grund för att mätningar kan genomföras kallas kärnämneskontroll eller *safeguards*. Alla använda kärnbränslen står under kärnämneskontroll och detta kontrolleras nationellt av Statens kärnkraftsinspektion, SKI, och internationellt av EU via Euratom och av FN via internationella atomenergiorganet, IAEA.

Kärnbränslet och dess egenskaper

Energin i ett kärnbränsleelement genereras genom att tunga kärnor såsom uran och plutonium klyvs till mindre delar, vanligen två nya mindre delar (klyvningsprodukter) samt 2 - 3 neutroner. Neutronerna är de de partiklar som klyver kärnorna och genom att kontrollera neutronerna ser man till att en kedjereaktion upprätthålls och en kontinuerlig energiproduktion fortgår.

Ungefär 500 bränsleelement utgör härden i en reaktor. Under klyningsprocessen utvecklas stora mängder värme i bränsleelementen och denna värme kokar vatten som omger alla bränslen i härden. Ångan från det kokande vattnet leds till en turbin som i sin tur genererar elektricitet som till slut matas ut till konsumenterna. Ett typisk från en kokvattenreaktor kärnbränsleelement kan ses i figur 8.1. Energin genereras huvudsakligen av de två uranisotoperna ^{235}U och ^{238}U men senare under bränslets livslängd även av plutonium. Mängden ^{235}U är anrikad till cirka 5% av det totala innehållet uran i ett bränsleelement. Denna typ av bränsle är den som används i de svenska reaktorerna. Man kan även göra bränslen med ett högt initialt plutoniuminnehåll, dessa brukar kallas för MOX-bränslen, då man har blandat uranoxid med plutoniumoxid. Dessa bränslen görs genom att återvinna det plutonium som har bildats i gamla använda kärnbränslen.

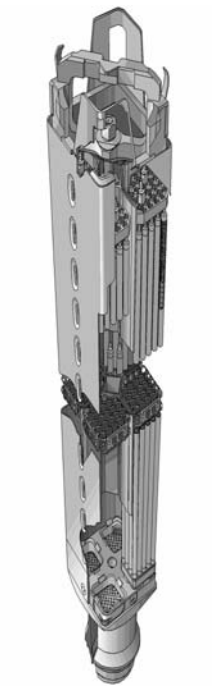

Figure 8.1: Ett kärnbränsleelement från en kokvattenreaktor. Bränslets längd är cirka 4 m med ett tvärsnitt om cirka $140 \times 140\,\mathrm{mm}^2$. Vikten är omkring 200 kg.

Ett bränsleelement är uppbyggt av kutsar av urandioxid som staplas på varandra i långa rör med cirka 1 cm diameter. Ett bränsle innehåller ett par hundra rör, beroende på bränslemodell. En reaktor körs i cykler om cirka 11 månader och stängs sedan av under ett par veckors tid då man gör översyn av rektorns tekniska delar och samtidigt byter ungefär 20% av alla bränsleelement mot nya. De gamla bränsleelementen förvaras sen i CLAB (Centralt mellanlager för använt kärnbränsle) i väntan på permanent djupförvaring. De använda bränslena innehåller klyvningsprodukter som bildats under energiproduktionen och som utsänder joniserande strålning. Denna strålning kan mätas och ur mätresultaten kan slusatser dras om bränslets egenskaper. Denna avhandling behandlar speciellt mätning av gammastrålning med gammaspektroskopiska metoder.

Gammaspektroskopi

För att mäta strålning så använder man sig av detektorer, för detta arbete har halvledardetektorer av germanium använts. Dessa har de egenskaperna att väldigt noggrant kunna mäta energin hos strålningen från de radioaktiva bränslena. På detta sätt får man en bra energiupplösning och man kan

då också säga från vilket ämne strålning med en viss energi kommer ifrån. För att mäta strålningen så placeras det använda kärnbränslet i en fixtur på väggen i hanteringsbassängen och strålningen tillåts sedan att passera en kollimator genom bassängväggen fram till detektorn som finns på andra sidan. Platsen där detektorn finns är ett torrt utrymme där också resten av den utrustnig man använder finns. Mätningarna i denna avhandling har uteslutande utförts på CLAB i Oskarshamn.

Metodernas tillämpningar

De ämnen som har studerats har varit ^{137}Cs, ^{134}Cs samt ^{154}Eu vilka enskilt och tillsammans kan berätta om bränslets olika egenskaper. De metoder som har utvecklats kan användas för att beräkna energiuttaget ur ett bränsle och bränslets kyltid (den tiden som bränslet stått utanför härden). Ett bränsle åtföljs alltid av dokumentation för hur bränslet har använts i härden (bestrålningshistoriken), anrikningsgrad av ^{235}U, effektuttaget samt andra bränsleegenskaper. Det är av intresse att kunna verifiera bestrålningshistoriken och på så sätt säkerställa att bränslet inte har körts i reaktorn på ett sätt som inte är förenligt med civil energiproduktion. En av metoderna i denna avhandling behandlar detta.

En metod har även utvecklats för att kunna skilja vanliga uranbränslen från MOX-bränslen om man förutsätter att allt annat är okänt.

Vid det framtida djupförvaret för använt kärnbränsle planerar man att kapsla in de använda bränsleelementen i kopparkapslar, cirka tio element per kapsel. Kapslarna ska sedan bäddas in i bentonitlera som buffer mot urberget och för att lera skall behålla sina egenskaper så får yttemperaturen på kapseln ej överstiga 100° C. Detta betyder i sin tur att bränslenas sammanlagda effekt ej får överstiga 1700 W och därför vill man mäta varje enskilt bränsles resteffekt. Detta kan göras genom att mäta hur mycket ^{137}Cs som varje bränsle innehåller eftersom ett nära samband existerar mellan mängden ^{137}Cs och bränslets resteffekt. Detta har också utretts i denna avhandling.

Bibliography

[1] http://www.iaea.org/OurWork/SV/Safeguards/index.html.

[2] A. Håkansson. A primer to safeguards and its instrumentation. Course compendium.

[3] http://www.iea.org.

[4] A. Koster, H.D. Matzner, and D.R. Nicholsi. PBMR design for the future. *Nuclear Engineering and Design*, 222:231 – 245, 2003.

[5] http://www.gen-4.org/.

[6] Uranium Information Centre. http://www.uic.com.au.

[7] SKB. Fud-program 2004, Programme for research, development and demonstration of methods for handling and final disposal of nuclear waste, including societal research, 2004.

[8] P.-E. Ahlström. Towards a swedish repository for spent fuel. *Nuclera Engineering and Design*, 176:67 – 74, 1997.

[9] K. Ikonen. Thermal analyses of spent nuclear fuel repository. Technical report, Posiva OY, 2003.

[10] Kenneth S. Krane. *Introductory Nuclear Physics*. John Wiley & Sons, 1988.

[11] S. Jacobsson Svärd. *A Tomographic Measurement Technique for Irradiated Nuclear Fuel Assemblies*. PhD thesis, Department of Radiation Sciences, Uppsala University, Sweden, 2004.

[12] G. Pfennig, H. Klewe-Nebenius, and W. Seelmann-Eggebert. Karlsruher nuklidkarte. *Forschunszentrum Karlsruhe*, 1998.

[13] S.M. Bowman and L.C. Leal. *ORIGEN-ARP: Automatic Rapid Process for Spent Fuel Depletion, Decay, and Source Term Analysis*, March 2000. NUREG/CR–0200.

[14] T.R. England and B.F. Rider. ENDF-349 Evaluation and Compilation of Fission Product Yields. Technical Report LA-UR-94-3106, Los Alamos National Laboratory, 1994.

[15] J.R. Philips, J.K. Halbig, D.M. Lee, E.E. Beach, T.R. Bement, E. Dermendjiev, C.R. Hatcher, K. Kaieda, and E.G. Medina. Application of Nondestructive Gamma-Ray and Neutron Techniques for the Safeguarding of Irradiated Fuel Materials. Report LA-8212 (ISPO-77), Los Alamos National Laboratory, 1980.

[16] R. Berndt. Verification of Spent PWR Fuel Data using the ^{154}Eu, ^{134}Cs and ^{137}Cs Activities. *Kernenergie*, 31:59–63, 1988.

[17] Ian Gauld. private communication.

[18] IAEA. Safeguards Techniques and Equipment, 2003. International Nuclear Verification Series No. 1 (Revised).

[19] P.M. Rinard and G.E. Bosler. Safeguarding LWR Spent Fuel with the Fork Detector. Technical Report LA-11096-MS (ISPO-281), Los Alamos National Laboratory, March 1988.

[20] P. Jansson. *Studies of Nuclear Fuel by Means of Nuclear Spectroscopic Methods*. PhD thesis, Department of Radiation Sciences, Uppsala University, Uppsala, Sweden, 2002.

[21] A. Bernstein, Y. Wang, G. Gratta, and T. West. Nuclear reactor safeguards and monitoring with antineutrino detectors, 2001. http://www.citebase.org/abstract?id=oai:arXiv.org:nucl-ex/0108001.

[22] Table of Isotopes. http://ie.lbl.gov/toi.htm.

[23] Aptec-NRC. *Series 5000 MCArd, Rev. 01*.

[24] Gordon Gilmore and John Hemingway. *Practical Gamma-Ray Spectrometry*. Wiley, 1995.

[25] M. Tarvainen, A. Bäcklin, and A. Håkansson. Calibration of the TVO spent BWR reference fuel assembly. Technical Report STUK-YTO-TR 37, Finnish Centre for Radiation and Nuclear Safety (STUK), 1992.

[26] O. Osifo. A data aquisition and analysis saoftware or verification of spent LWR fuel parameters at an encapsulation plant. To be submitted to Nuclear Instruments and Methods in Physics Research.

[27] T.D. Reilly and J.L. Parker. A Guide to Gamma-Ray Assay for Nuclear Material Accountability. Technical Report LA-5794-M, Los Alamos Scientific Laboratory, 1975.

[28] C.E. Sanders and I.C. Gauld. Isotopic Analysis of High-Burnup PWR Spent Fuel Samples From the Takahama–3 Reactor. Technical Report ORNL/TM-2001/259, Oak Ridge National Laboratory, 2003.

[29] Studsvik Energiteknik AB. SIMULATE-3. Advanced Three-Dimensional Two-Group Reactor Analysis Code, 1995. STUDSVIK/SOA-95/15-REV 0.

[30] M. Edenius, K. Ekberg, B.H. Forssen, and D. Knott. CASMO-4, A Fuel Assembly Burn-up Program: User's Manual, 1995. STUDSVIK/SOA-95/1.

[31] P.R. Thorne, G.J. O'Connor, and R.L. Bowden. Problem Specifications for the OECD/NEANSC Burnup Credit Benchmark Phase IV-B: Mixed Oxide (MOX) Fuels. Technical report, Safety & Environment Risk Management, BNFL, 2002.

[32] International Atomic Energy Agency. Status and advances in MOX fuel technology. Technical Report no. 415, IAEA, 2003. ISSN 0074–1914.

[33] IAEA. IAEA Coordinated Technical Meeting on Spent Fuel Verification Methods. 2003.

[34] P. Jansson and A. Håkansson and A. Bäcklin and S. Jacobsson. Gamma-ray spectroscopy measurements of decay heat in spent nuclear fuel. *Nuclear Science and Engineering*, 141(2), 2002.

[35] F. Robelius. *Giant oil fields and their importance for peak oil*. Uppsala university, 2005. Licentiate thesis.

[36] B. Andersson and B. Grapengiesser. Measurements on Fuel Assemblies from Cofrentes for Determination of Relative Power Distribution. Technical Report 02-169, Westinghouse Atom AB, 2002.

[37] S. Jacobsson, C. Andersson, A. Håkansson, and A. Bäcklin. A Tomographic Method for Verification of the Integrity of Spent Nuclear Fuel Assemblies – I: Simulation Studies. *Nuclear Technology*, 135(2):131–145, 2001.

[38] S. Jacobsson, A. Håkansson, P. Jansson, and A. Bäcklin. A Tomographic Method for Verification of the Integrity of Spent Nuclear Fuel Assemblies – II: Experimental Investigation. *Nuclear Technology*, 135(2):146–153, 2001.

[39] A. Fritzell. Concerns when designing a safeguards approach for the back-end of the swedish fuel cycle. Master's thesis, Uppsala Univeristy, 2006.

Acta Universitatis Upsaliensis

Digital Comprehensive Summaries of Uppsala Dissertations from the Faculty of Science and Technology 212

Editor: The Dean of the Faculty of Science and Technology

A doctoral dissertation from the Faculty of Science and Technology, Uppsala University, is usually a summary of a number of papers. A few copies of the complete dissertation are kept at major Swedish research libraries, while the summary alone is distributed internationally through the series Digital Comprehensive Summaries of Uppsala Dissertations from the Faculty of Science and Technology. (Prior to January, 2005, the series was published under the title "Comprehensive Summaries of Uppsala Dissertations from the Faculty of Science and Technology".)

Distribution: publications.uu.se
urn:nbn:se:uu:diva-7116

ACTA
UNIVERSITATIS
UPSALIENSIS
UPPSALA
2006